2004-06

Improved method for simulating total radiation dose effects on single and composite operational amplifiers using PSPICE

Dufour, David M.

Monterey California. Naval Postgraduate School

NAVAL POSTGRADUATE SCHOOL

MONTEREY, CALIFORNIA

THESIS

IMPROVED METHOD FOR SIMULATING TOTAL RADIATION DOSE EFFECTS ON SINGLE AND COMPOSITE OPERATIONAL AMPLIFIERS USING PSPICE

by

David M. Dufour

June 2004

Thesis Advisor:	Sherif N. Michael
Second Reader:	Andrew A. Parker

Approved for public release; distribution is unlimited

THIS PAGE INTENTIONALLY LEFT BLANK

REPORT DOCUMENTATION PAGE			Form Approved OMB No. 0704-0188
Public reporting burden for this collection of information is estimated to average 1 hour per response, including the time for reviewing instruction, searching existing data sources, gathering and maintaining the data needed, and completing and reviewing the collection of information. Send comments regarding this burden estimate or any other aspect of this collection of information, including suggestions for reducing this burden, to Washington headquarters Services, Directorate for Information Operations and Reports, 1215 Jefferson Davis Highway, Suite 1204, Arlington, VA 22202-4302, and to the Office of Management and Budget, Paperwork Reduction Project (0704-0188) Washington DC 20503.			
1. AGENCY USE ONLY ***(Leave blank)***	**2. REPORT DATE** June 2004	**3. REPORT TYPE AND DATES COVERED** Master's Thesis	
4. TITLE AND SUBTITLE: Improved Method for Simulating Total Radiation Dose Effects on Single and Composite Operational Amplifiers Using PSPICE			**5. FUNDING NUMBERS**
6. AUTHOR(S) David M. Dufour			
7. PERFORMING ORGANIZATION NAME(S) AND ADDRESS(ES) Naval Postgraduate School Monterey, CA 93943-5000			**8. PERFORMING ORGANIZATION REPORT NUMBER**
9. SPONSORING /MONITORING AGENCY NAME(S) AND ADDRESS(ES) N/A			**10. SPONSORING/MONITORING AGENCY REPORT NUMBER**
11. SUPPLEMENTARY NOTES The views expressed in this thesis are those of the author and do not reflect the official policy or position of the Department of Defense or the U.S. Government.			
12a. DISTRIBUTION / AVAILABILITY STATEMENT Approved for public release, distribution is unlimited			**12b. DISTRIBUTION CODE**

13. ABSTRACT (maximum 200 words)

This research is part of a continued effort to simulate the effects of total dose radiation on the performance of single and composite operational amplifiers using PSPICE. This research provides further verification that the composite operational amplifier has a superior performance to the single operational amplifier while operating in a radiation flux. In this experiment, a single and composite op amp were constructed in PSPICE and implemented in a finite gain amplifier circuit. The effects of ionizing radiation were simulated by varying the parameters of the components that made up the op amps. These component parameters were varied in ways that would mimic the response of the actual components that were irradiated in previous research. The simulations were incrementally run to simulate an increasing radiation dose. The results of these simulations were then compared with the results of an actual study conducted at Naval Postgraduate School where similar circuits were irradiated using the school's LINAC. This procedure proved to be an improved method for predicting the effects of total dose radiation for radiation hardened devices and provided additional confirmation of the superior performance of the composite op amp over the single op amp.

14. SUBJECT TERMS PSPICE, LINAC, Op Amp, Single and Composite Operational Amplifiers, Finite Gain Amplifier Circuit			**15. NUMBER OF PAGES** 99
			16. PRICE CODE
17. SECURITY CLASSIFICATION OF REPORT Unclassified	**18. SECURITY CLASSIFICATION OF THIS PAGE** Unclassified	**19. SECURITY CLASSIFICATION OF ABSTRACT** Unclassified	**20. LIMITATION OF ABSTRACT** UL

NSN 7540-01-280-5500

Standard Form 298 (Rev. 2-89)
Prescribed by ANSI Std. 239-18

THIS PAGE INTENTIONALLY LEFT BLANK

Approved for public release; distribution is unlimited

IMPROVED METHOD FOR SIMULATING TOTAL RADIATION DOSE EFFECTS ON SINGLE AND COMPOSITE OPERATIONAL AMPLIFIERS USING PSPICE

David M. Dufour
Lieutenant, United States Navy
B.S., Chapman University, 1995

Submitted in partial fulfillment of the
requirements for the degree of

MASTER OF SCIENCE IN ELECTRICAL ENGINEERING

from the

NAVAL POSTGRADUATE SCHOOL
June 2004

Author: David M. Dufour

Approved by: Sherif N. Michael
Thesis Advisor

Andrew A. Parker
Second Reader

John P. Powers
Chairman, Department of Electrical and Computer Engineering

THIS PAGE INTENTIONALLY LEFT BLANK

ABSTRACT

This research is part of a continued effort to simulate the effects of total dose radiation on the performance of single and composite operational amplifiers using PSPICE. This research provides further verification that the composite operational amplifier has a superior performance to the single operational amplifier while operating in a radiation flux. In this experiment, a single and composite op amp were constructed in PSPICE and implemented in a finite gain amplifier circuit. The effects of ionizing radiation were simulated by varying the parameters of the components that made up the op amps. These component parameters were varied in ways that would mimic the response of the actual components that were irradiated in previous research. The simulations were incrementally run to simulate an increasing radiation dose. The results of these simulations were then compared with the results of an actual study conducted at Naval Postgraduate School where similar circuits were irradiated using the school's LINAC. This procedure proved to be an improved method for predicting the effects of total dose radiation for radiation hardened devices and provided additional confirmation of the superior performance of the composite op amp over the single op amp.

THIS PAGE INTENTIONALLY LEFT BLANK

TABLE OF CONTENTS

I. INTRODUCTION....1

II. SPACE AND THE RADIATION ENVIRONMENT....5
- A. PHOTON RADIATION....5
  - 1. Photoelectric Effect....5
  - 2. Compton Scattering Effect....6
  - 3. Pair Production....7
- B. PARTICLE RADIATION....8
  - 1. Beta Particles....9
  - 2. Alpha Particle....9
  - 3. Positron Radiation....10
  - 4. Neutron Radiation....11
- C. THE RADIATION ENVIRONMENT OF SPACE....11
  - 1. Cosmic Rays....12
  - 2. Solar Plasma....13
  - 3. Van Allen Belts....14
- D. RADIATION EFFECTS....15
  - 1. Ionization Damage....15
  - 2. Displacement Damage Effects....16
  - 3. Transient Damage Effects....16
  - 4. Surface Damage Effects....16
  - 5. Annealing....17

III. SEMICONDUCTOR DEVICES....19
- A. BIPOLAR JUNCTION TRANSISTORS....19
  - 1. Emitter Current....20
  - 2. Base Current....21
  - 3. Collector Current....21
  - 4. Collector-Base Reverse Current....21
  - 5. Current Gain....21
  - 6. Radiation Effects on the BJT....22
- B. CAPACITOR....24
  - 1. Dielectric....24
- C. RADIATION EFFECTS ON THE CAPACITOR....25

IV. SINGLE AND COMPOSITE OPERATIONAL AMPLIFIERS....29
- A. THE 741 OPERATIONAL AMPLIFIER....29
  - 1. The Bias Circuit....31
  - 2. The Input Stage....31
  - 3. The Second Stage....32
  - 4. The Output Stage....33
  - 5. The Short Circuit Protection Circuit....34
- B. THE COMPOSITE OPERATIONAL AMPLIFIER....35

C. COMPOSITE OP AMP THEORY 35
D. RADIATION EFFECTS ON SINGLE AND COMPOSITE OP AMPS ..36
V. SIMULATION PROCEDURE 43
A. BACKGROUND 43
B. SIMULATION SET-UP 45
C. RADIATION SIMULATION 46
1. Transistor Correlation 46
2. Capacitor Correlation 47
D. SIMULATION PROCEDURE 48
E. OUTPUT BASELINE 50
VI. RESULTS 53
A. OBJECTIVES 53
B. BASELINE FOR COMPARISON 57
C. SINGLE OP AMP COMPARISON 57
D. COMPOSITE OP AMP COMPARISON 59
E. C2OA1 AND SINGLE OP AMP (SOA) COMPARISONS 61
VII. CONCLUSIONS AND RECOMMENDATIONS 65
A. SINGLE OP AMP CONCLUSIONS 65
B. COMPOSITE OP AMP CONCLUSIONS 65
C. SUPPORTING OBSERVATIONS 66
D. BANDWIDTH COMPARISON OF C2OA1 AND SOA CIRCUITS 66
E. RECOMMENDATIONS 66
APPENDIX. EXPERIMENT DATA 69
LIST OF REFERENCES 77
INITIAL DISTRIBUTION LIST 81

LIST OF FIGURES

Figure 2.1. Photoelectric Effect [From Ref. 6.] 6
Figure 2.2. Compton Scattering [From Ref. 6.] 7
Figure 2.3. Pair Production [From Ref. 6.] 8
Figure 2.4. Beta Particle Radiation [From Ref. 6.] 9
Figure 2.5. Alpha Particle Radiation [From Ref. 6.] 10
Figure 2.6. Positron Radiation [From Ref. 6.] 11
Figure 2.7. Cosmic Ray Shower [From Ref. 12.] 12
Figure 2.8. Solar Wind and Magnetosphere [From Ref. 13.] 14
Figure 2.9. Van Allen Belts [From Ref. 12.] 15
Figure 3.1. Current Flow of an Active Biased PNP BJT [From Ref. 4.] 20
Figure 3.2. Effects of Total Rad Dose on β for Two Test Transistors [From Ref. 17.] 23
Figure 3.3. Effects of Total Rad Dose on β for Two Test Transistors [From Ref. 17.] 23
Figure 3.4. Effects of Total Rad Dose on β for Four Test Transistors [From Ref. 17.] 24
Figure 3.5. Metal Oxide Capacitor [From Ref. 26.] 25
Figure 3.6. Low-Pass Filter [From PSPICE.] 26
Figure 3.7. Capacitance vs. Total Rad Dose [From Ref. 20.] 27
Figure 4.1. 741 Op Amp [From PSPICE.] 29
Figure 4.2. 741 Operational Amplifier [From Ref. 4.] 30
Figure 4.3. Input Stage [From Ref. 27.] 32
Figure 4.4. Second Stage [From Ref. 27.] 33
Figure 4.5. Output Stage [From Ref. 27.] 34
Figure 4.6. Short Circuit Protection [From Ref. 27.] 35
Figure 4.7. Superior C2OA Configurations [From Ref. 5.] 37
Figure 4.8. C2OA1 Composite Op Amp [From Ref. 5.] 38
Figure 4.9. 3-dB Frequency % Change of Non-Radiation Hardened Single and Composite Op Amps [From Ref. 5.] 39
Figure 4.10. Gain % Change for Non-Radiation Hardened Single and Composite Op Amps [From Ref. 5.] 40
Figure 4.11. 3-dB Frequency % Change for Rad-Hardened Single and Composite Op Amps [From Ref. 5.] 40
Figure 4.12. Gain % Change for Rad-Hardened Single and Composite OP Amps [From Ref. 5.] 41
Figure 4.13. 3-dB Frequency of Rad-Hardened Single and Composite Op Amps [From Ref. 5.] 41
Figure 5.1. Normalized β Measurements vs. Total Rad Dose [From Ref. 3.] 43
Figure 5.2. Results from Single Op Amp Simulations [From Ref. 3.] 44
Figure 5.3. Results from C2OA1 Simulations [From Ref. 3.] 45
Figure 5.4. Comparison of the Actual Test Chip Values to the Predicted Compensating Capacitance Values Used for this Simulation 48
Figure 5.5. PSPICE Model of the Single Op Amp in the Finite Gain Amplifier Circuit [From PSPICE] 49

Figure 5.6. PSPICE Model of the Composite Op Amp Configured in a Finite Gain Amplifiers Circuit [From PSPICE] 50
Figure 6.1. Single and Composite Op Amp Gain Comparison 54
Figure 6.2. Single and Composite Op Amp Gain % Comparison 54
Figure 6.3. Simulated Single and Composite Op Amp 3-dB Frequency Comparison 55
Figure 6.4. Simulated Single and Composite Op Amp 3-dB Frequency % Comparison 55
Figure 6.5. Single and Composite Op Amp Gain Bandwidth Product Comparison 56
Figure 6.6. Single and Composite Op Amp Gain Bandwidth Product Percentage Comparison 56
Figure 6.7. Single Op Amp Actual and Simulated Gain (%) Comparison 58
Figure 6.8. Single Op Amp Actual and Simulated 3-dB Frequency Comparison 58
Figure 6.9. Single Op Amp Actual and Simulated 3-dB (%) Frequency Comparison 59
Figure 6.10. Gain Percentage Comparison for the Actual and Simulated Irradiated C2OA1 60
Figure 6.11. 3-dB Frequency Comparison for the Actual and Simulated Irradiated C2OA1 60
Figure 6.12. 3-dB Frequency Percentage for the Actual and Simulated C2OA-1 61
Figure 6.13. SOA and C2OA1 Gain Comparisons 62
Figure 6.14. SOA and C2OA1 3-dB Frequency Comparisons 63
Figure 6.15. C2OA and SOA GBWP Comparison 63

LIST OF TABLES

Table 2.1. Summary of Radiation Effects on Semiconductor Devices [From Ref. 15.]...17
Table 3.1. BJT Modes of Operation [From Ref. 4].....20
Table 5.1. Transistor Parameters [From Ref. 3.] 46
Table 5.2. Capacitance Values Before and After 2.399 Mrad (Si) Dose.....47
[From Ref. 20.] 47

THIS PAGE INTENTIONALLY LEFT BLANK

ACKNOWLEDGMENTS

I would like to thank my advisor, Dr. Sherif Michael for his invaluable encouragement, guidance and supervision through the Naval Postgraduate School. I would also like to thank Professor Andrew Parker for his generous counsel and support, and Jeffery Knight for keeping the electronics lab always up and running.

THIS PAGE INTENTIONALLY LEFT BLANK

EXECUTIVE SUMMARY

The need for instantaneous global communications has become essential not only for international business but for the Department of Defense. The infrastructure required to provide this capability involves the extensive use of satellites. The cost of building a satellite that can survive the harsh radiation environment of space and to launch it into orbit has grown exponentially over the decades. Particular interest has gone into techniques to reduce the cost of these satellites while improving their performance in a radiation environment. This study is part of a continued effort to simulate the effects of total dose radiation on the performance of single and composite operational amplifiers using MicroSim's® simulation software PSPICE, Release 8.

This study commenced with researching the different types of radiation and their sources. The study continued by researching the components that are used to construct the operational amplifier such as the bipolar junction transistor (BJT) and the capacitor. The effects of radiation on these individual components were also examined. Single and composite operational amplifier theory was investigated along with the effects of radiation on those two circuits.

Based on the research conducted, a correlation between the component parameters and total radiation dose was established. The PSPICE simulations were performed by varying the individual components parameters of the transistors and capacitors that made up the op amp circuits while running the tests. The results of these simulations were compared to the results of actual experiments conducted at Naval Postgraduate School using similar circuits. The comparisons were remarkably close illustrating that the effects of total dose radiation on the compensating capacitor has a dramatic effect on the 3-dB frequency and the gain bandwidth product of both the single and composite op amp. This study took us a step closer to simulating the effects of radiation on op amps and shows promise for further research and improvements in that endeavor.

THIS PAGE INTENTIONALLY LEFT BLANK

I. INTRODUCTION

The information age of the 1990's has evolved into an age where global communications is routine and is often taken for granted. The infrastructure required to provide this capability involves the use of satellites. From their inception in the United States in the early 1960's to the present, communication satellites have steadily become the backbone for global communications not only in the commercial sector but more importantly, the Department of Defense. The cost of putting a satellite in orbit can be astronomical. In the 1980's the average cost of a communication satellite was $80 million, which included the cost to launch it into space. The Hubble telescope initially cost $1.5 billion to build and launch into orbit. The Hubble had an additional cost of $8 million to make repairs to it in space before it could finally become operational. [Ref. 1] Due to the increasing cost of satellites, particular interest has gone into techniques to improve their performance and prolong their life expectancy while operating in the harsh thermal and radiation environment of space.

The first of these techniques is to thicken the side panels of the components themselves. This provides some protection by absorbing the radiation energy, but adds additional bulk to these components. A second technique involves applying radiation shielding to the components or circuits themselves. These techniques decrease radiation exposure, but may be deemed impractical for some uses. Thickening side panels and additional shielding increases the bulk and the weight of these components, which in turn increases the bulk and weight of the spacecraft, increasing the cost to put it into space. The average cost per pound to put a satellite in low earth orbit (LEO) ranges between $3,600 and $4,900. To put a satellite in further out into geo-stationary orbit (GEO), the cost per pound increases from $9,200 to $11,200. [Refs. 2, 3, 25]

A third technique is a manufacturing process that produces electronic components that are radiation hardened (rad hard). Some examples of rad hardening techniques used by manufacturers include dielectric isolation, silicon on insulator (SOI), silicon on sapphire (SOS), and higher gate complexity. [Ref.3] Rad hard components are usually guaranteed to perform to specific standards when irradiated to given levels and rates of radia-

tion exposure. Of the three techniques discussed, rad hardened components are the most cost efficient means to combat the effects of radiation on the performance of the op amp; however, these components are usually expensive and could require an extensive budget to incorporate into satellite applications. [Refs. 2, 3]

A fourth option is a technique known as radiation tolerant or rad tolerant devices. Rad tolerant techniques use components that can be inherently sensitive to the effects of radiation, but are arranged in unique circuits that make their system sensitivity to the effects of radiation less apparent. [Ref. 3] This technique is even less expensive than rad hardening because less emphasize is placed on the costly production process. This makes radiation tolerant devices less expensive but the components themselves are still susceptible to the effects of radiation and therefore less reliable than rad hardened components. [Ref. 3]

The operational amplifier, or op amp, because of its diversity of uses, is a frequently used building block in many electronic circuits in satellites. The typical op amp is a multistage differential amplifier constructed from several semiconductor devices which can be rad hardened to protect the op amp from the effects of radiation. The effects of radiation have been shown to have a detrimental effect on the performance of the op amp even if they are rad hardened. [Ref. 3] The degraded performance of the op amp translates to the degraded performance of the circuits that employ them. The gain and 3-dB frequency of an op amp placed in a finite-gain amplifier circuit can be significantly degraded. Placing these op amps in a rad tolerant configuration is an additional method that can be used to lessen the effects of radiation of these circuits. [Ref. 3]

A derivative of the op amp, known as the composite op amp, is a circuit composed of two or more op amps placed in a special cascaded arrangement to provide a circuit that performs like an op amp, but provides an improved performance over that of the single op amp. [Ref. 3] Research conducted by Sherif Michael and Wasfy Mikhael in 1981 identified 136 different composite op amps composed of two single op amps. [Refs. 3, 5] From their research, it was hypothesized that composite op amps have radiation tolerant properties over single op amps. This study focused on exploring techniques for simulating the effects of radiation on the single op amp and composite op amp in an ef-

fort to allow design engineers to model and test these circuits at their conception before they are manufactured. This ability will ultimately save time and money in designing electronic circuits to be used in satellites or any other electronic circuit that is expected to operate in the harsh radiation environment of space or in a nuclear radiation environment. [Refs. 3, 5]

This thesis is a continued study on the attempts to simulate the effects of radiation on the op amp and the composite op amp. In a previous study, the op amp and composite op amp were modeled in PSPICE and simulated to operate in a radiation flux. To simulate the effects of radiation on these circuits, the value of the current gain designated as β was varied accordingly in every transistor in these circuits. The circuits were simulated and the results were compared to that of actual op amps, configured in the same type of circuit and irradiated using the linear accelerator (LINAC) at Naval Postgraduate School. [Refs. 3, 5]

In this continued research, the single and composite BJT op amps were simulated in the same circuits as above, but additional op amp parameters were varied to mimic the effects of radiation on these circuits. The value of β was again varied as in the previous experiment, and the values of internal compensating capacitance were varied to reflect the effects of total dose exposure. The simulations were run, and the data collected were compared with the results from actual experiments conducted with the same type of circuits at Naval Postgraduate School.

Chapter II discusses the various types of radiation that exists in the space environment and the typical effects that this radiation has on electronic devices.

Chapter III provides a general overview of general silicon devices that make up the major electronic components of the operational amplifier and the effects of radiation on those devices.

Chapter IV views the combination of these components as a whole to function as an operational amplifier and a composite operational amplifier. This chapter further discusses the effects of radiation on the single op amp and composite op amp as a whole.

Chapter V describes the set-up of the method for simulating the effects of radiation on the single and composite op amps.

Chapter VI presents the results of the simulations that were run.

Chapter VII offers the conclusions from the simulated experiments conducted and offers recommendations that may improve the next set of experiments.

II. SPACE AND THE RADIATION ENVIRONMENT

In today's world, fast and reliable communications is a must and is often taken for granted. Communication satellites are a vital segment of the communications infrastructure and their reliability in the harsh environment of space cannot be understated. Satellites and other spacecrafts launched into space are exposed to various forms of radiation. It is important for the design engineer when designing these spacecraft to understand the properties of the radiation and its effect on electronic components. Countering the effects of radiation on semi-conductor devices can improve the performance of the circuits and prolong the life expectancy of the spacecraft. To first understand the effects of radiation it is important to understand the types of radiation that the spacecraft may be exposed to. The radiation environment of space can be generally categorized as photons or particles.

A. PHOTON RADIATION

Photons are particle representations of electromagnetic waves, which are composed of discrete quanta of electromagnetic energy. [Ref. 6] The most significant types of photon radiation are X-rays and Gamma rays. X-rays and Gamma rays are distinguished from one another by their origins. X-rays are generated by energetic electron processes, while Gamma rays are generated by transitions within the atomic nuclei. [Ref. 6] Gamma rays are higher in energy and have higher penetrating power than X-rays. Photons have no mass and have a neutral charge but do react with matter when they come in contact. [Ref. 6] The energy of a photon can be described with the expression $h\upsilon$, where h is Planck's constant ($6.626\times10^{-34}\,\mathrm{J\cdot s}$) and the variable υ represents the frequency of the electromagnetic wave. [Ref. 6] Although photons are massless, they do behave like particles when they come in contact with matter. [Ref. 6] The three types of interactions are called Photoelectric effect, Compton scattering effect, and pair production.

1. Photoelectric Effect

The photoelectric effect takes place when the energy of the photon is completely transferred to an orbital electron which is ejected from its atom, as illustrated in Figure 2.1. [Ref. 6] With the photoelectric effect, the energy of the photon $(h\upsilon)$ is completely absorbed by the atom and its electron and will no longer exist. [Ref. 6] This effect

normally takes place when the atom is exposed to the energy level of a Gamma ray or an X-ray. [Ref. 6] The ejected electron could then cause ionization in other atoms until it loses its energy and is captured by another atom. [Ref. 6] The photoelectric effect is more likely to occur when the energy of the photon is low, i.e. below 0.5 MeV and the absorber is a dense substance. [Ref. 6]

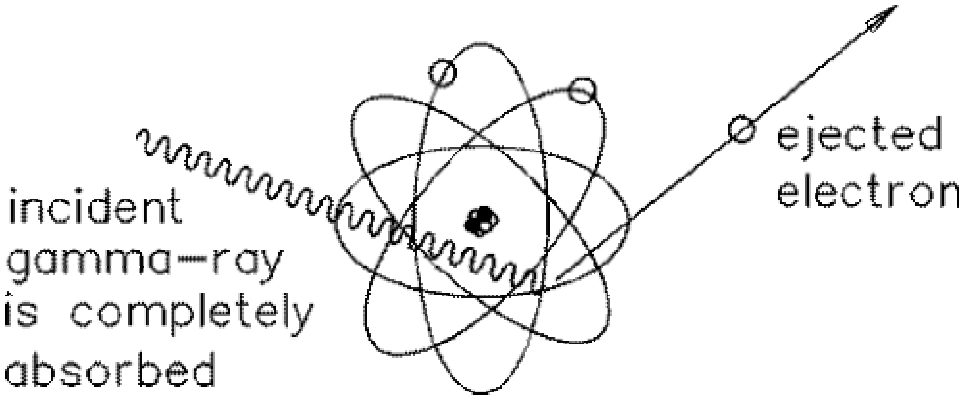

Figure 2.1. Photoelectric Effect [From Ref. 6.]

2. Compton Scattering Effect

When the photon energy is higher, about 0.5 to 3.5 MeV, the photon may cause an effect called Compton Scattering (Figure 2.2). [Ref. 6] The photon may lose only part of its energy ejecting the electron from its atom. This electron could go on to create ionization in other atoms. The remaining incident electromagnetic energy is transformed into another photon of lower frequency (υ) and reduced energy which is scattered in a new direction. [Ref. 6] The scattered photon may continue Compton scattering in other atoms if it has sufficient energy or will be absorbed by the photoelectric effect. [Ref. 6] "Compton scattering occurs in all materials and predominantly with photons of medium energy, i.e., about 0.5 to 3.5 MeV." [Ref. 6]

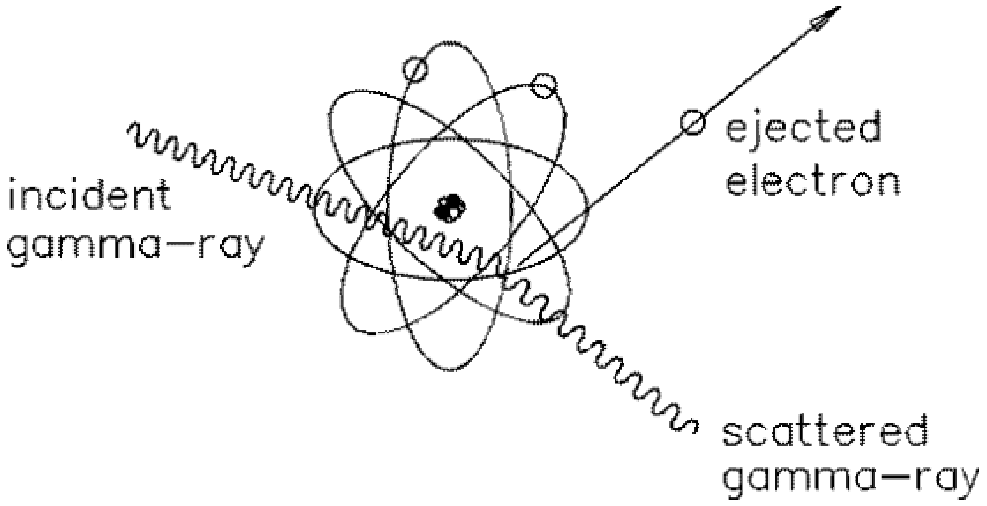

Figure 2.2. Compton Scattering [From Ref. 6.]

3. Pair Production

Photons with electromagnetic energy greater than 1.02 MeV may collide with a nucleus to form an electron-positron pair. [Ref. 6] This effect is called pair production (see Figure 2.3). The positron is a particle which has a mass equal to that of the electron. It has a positive electric charge equal in value to the negative charge of the electron. [Ref 6] This energy from the incident photon will be equally divided between the masses of the electron and positron (0.51 MeV each). "Excess energy will be carried away equally by these two particles which produce ionization as they travel in the material." [Ref. 6] The positron and electron eventually come together and the two particles are annihilated. "This results in the release of two photons each of 0.51 MeV known as annihilation radiation." [Ref. 6] These two photons then continue to cause Compton scattering or the photoelectric effect until their energy is spent.

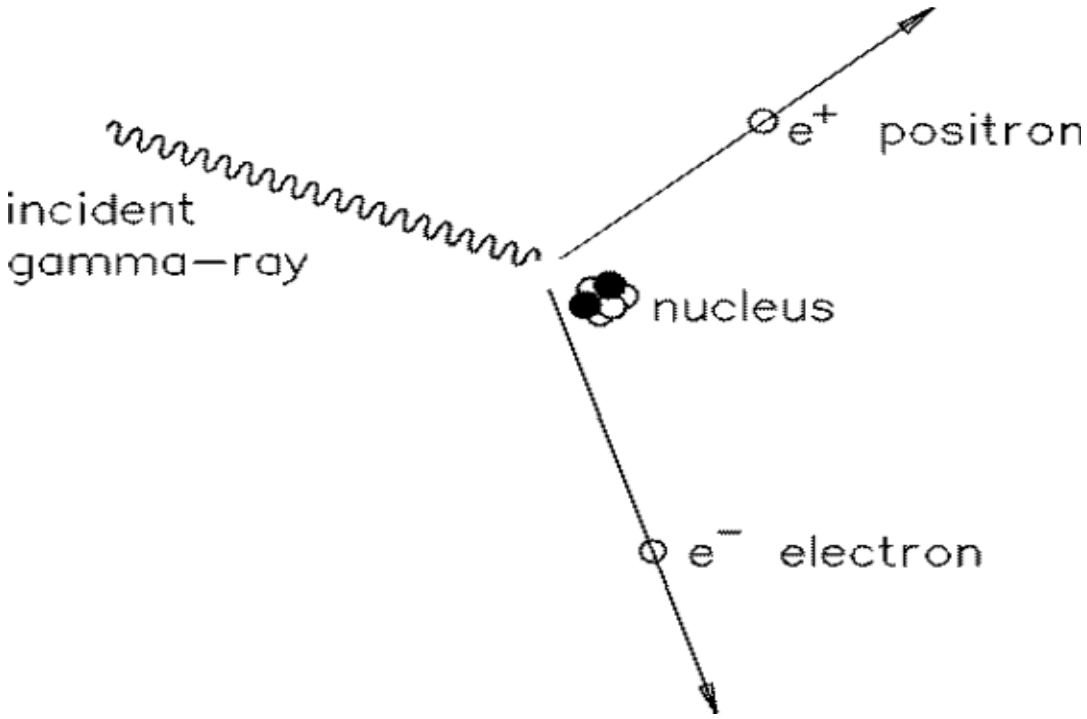

Figure 2.3. Pair Production [From Ref. 6.]

B. PARTICLE RADIATION

All known elements consist of protons, neutrons, and electrons. Protons carry a positive charge. The number of protons in the nucleus of the atom is called the atomic number and determines the identity of that atom. [Ref. 6] Electrons carry a negative charge. The atomic number also indicates the number of electrons in the neutral atom. Neutrons do not carry a charge and do not add to the atomic number of the atom. Neutrons do add to the atomic mass of an atom and have an effect on the stability of the nucleus of the atom. [Ref. 6]

It is known that, at a distance, like charges repel each other. The like electrical charges of the protons in the atom's nucleus are held together by the nuclear force of attraction, which is strong enough at close distances to overcome the repelling force of like charges and hold the atom together. [Ref. 6] Neutrons increase the stability of the nucleus by adding to the nuclear force of attraction without adding to the electrical force of repulsion. [Ref. 6] "A nucleus which has too many or too few neutrons for its number of protons will be unstable and may spontaneously rearrange its constituent particles to

form a more stable nucleus." [Ref. 6] During this process one or more particles may be emitted from the nucleus, such as beta particles, positrons, alpha particles, and if very far from stability even neutrons and protons. [Refs. 6, 7]

1. Beta Particles

Beta particles are high-energy electrons. "If a nucleus has too many neutrons the most likely form of decay will be the emission of an electron from the nucleus." [Ref. 6] Electrons do not exist independently in the nucleus. The beta particle forms when a neutron is transformed instantaneously into a proton and an energetic electron, which is ejected from the nucleus. [Ref. 6] The beta particle is very light. Its mass is about 1/2000 that of the proton; therefore they ionize less easily than heavy particles but they have a much longer range. [Ref. 7] The example in Figure 2.4 shows that one of the neutrons of tritium ${}^{3}H$ is instantly transformed to a proton because of instability. This transformation releases a photon and an electron is ejected from the nucleus. The tritium atom is transformed to ${}^{3}He$. [Ref. 6, 7]

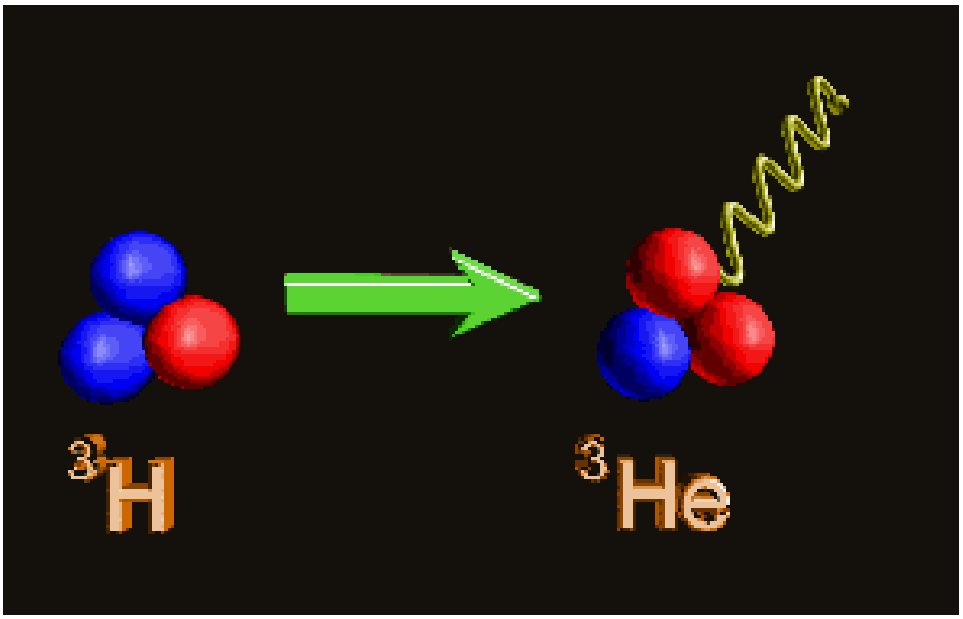

Figure 2.4. Beta Particle Radiation [From Ref. 6.]

2. Alpha Particle

The alpha particle is a fast moving helium nucleus consisting of two protons and two neutrons. [Ref. 6] It is about 8000 times heavier than an electron and has twice the

electric charge. [Ref. 7] The alpha particle produces heavy ionization per centimeter of travel, but its energy is expended quickly so it travels very short distances and has very little penetrating power. [Ref. 6] Travel distances in air are only a few centimeters. In solid matter the distance is only a few hundredths of a millimeter. [Refs. 6, 7] Figure 2.5 provides an example of alpha particle radiation as a helium atom is ejected from an atom of Americium producing Neptunium. [Refs. 6, 7]

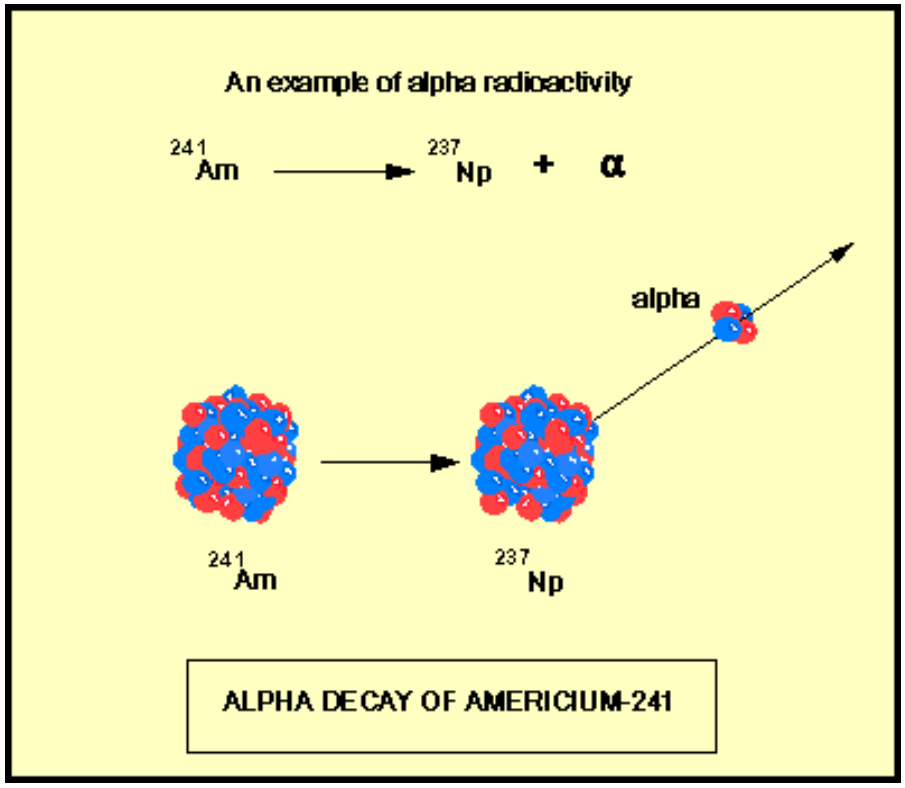

Figure 2.5. Alpha Particle Radiation [From Ref. 6.]

3. Positron Radiation

A positron is the antimatter equivalent of the electron. It has the same mass as an electron but has the equivalent positive charge. [Ref. 6] A positron may be generated by positron emission radioactive decay or beta + decay. In beta + decay a proton is converted to a neutron and a positron particle is emitted. Positron emission radioactive decay occurs during the interaction of photons of energy greater than 1.022 MeV with

matter. [Ref.6] As discussed earlier, this process is called pair production, as it generates both an electron and a positron from the energy of the photon. Figure 2.6 provides an example of positron radiation. [Refs. 6, 7]

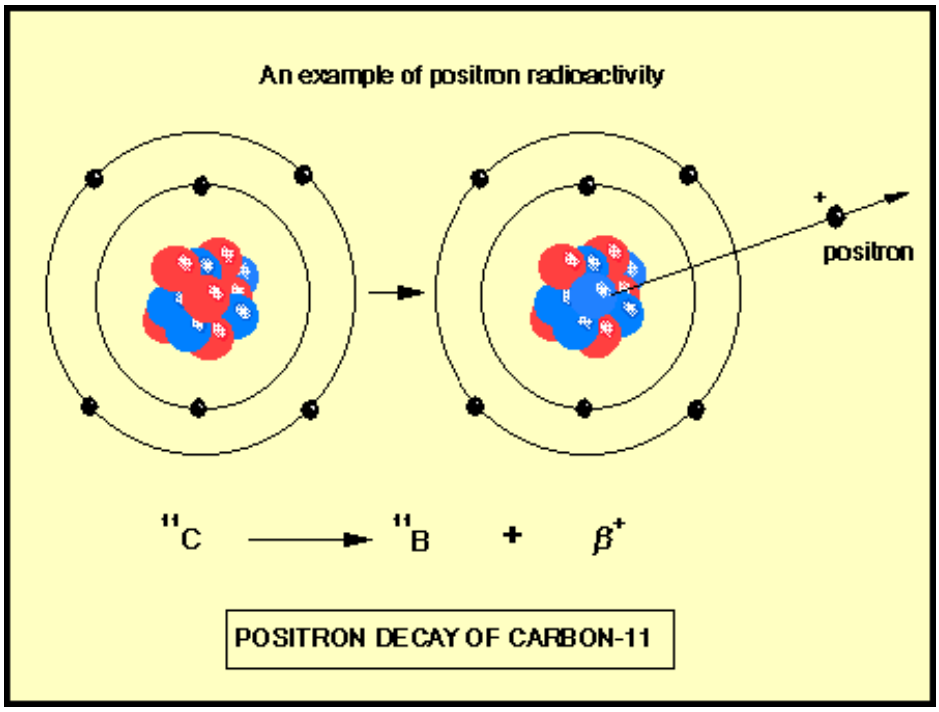

Figure 2.6. Positron Radiation [From Ref. 6.]

4. Neutron Radiation

Neutron radiation is usually produced by nuclear reactions such as fission, fusion, or a nuclear yield. [Ref. 3] Neutron radiation does occur in space and can cause significant radiation damage. The neutron has the same mass as a proton but with no electric charge. Because the neutron has no electric charge, it is not influenced by magnetic fields so is hard to stop and has high penetrating power. [Refs. 6, 7]

C. THE RADIATION ENVIRONMENT OF SPACE

Space presents an interesting challenge for the electrical engineer. When designing electronic circuits that will be incorporated into satellites and other spacecraft, it is important to understand the radiation environment that these circuits will be expected

to operate in. Radiation exists naturally in space. Radiation can fundamentally be broken down into photons and particle radiation. The main sources of radiation in space come from comic rays, solar plasma, or the Van Allen Belts.

1. Cosmic Rays

Cosmic rays were discovered in 1912 by Victor Hess. [Ref. 9] Hess placed an electroscope into a balloon and as it ascended, he found that the electroscope discharged more rapidly as it ascended. He determined that this reaction was caused by a source of radiation that entered the atmosphere from space. [Ref. 9] In 1936, Hess was awarded the Nobel Prize for his discovery. "Cosmic rays are high-energy charged particles, originating in outer space that travel at nearly the speed of light and strike the Earth from all directions." [Ref. 9] When the particles in the cosmic rays collide with particles in the earth's atmosphere, they disintegrate into smaller particles called pions and muons. This process is called a cosmic ray shower and is depicted in Figure 2.7. [Ref. 12] Cosmic rays are mostly made up from the nuclei of atoms, ranging from the lightest to the heaviest elements in the periodic table. [Ref. 9] Cosmic rays also include high-energy electrons, positrons, and other subatomic particles. Cosmic rays can be classified as galactic or solar depending on their origin. Galactic cosmic rays originate from the Milky Way galaxy and other distant unidentified sources in space. [Ref. 9] Galactic cosmic rays constitute the majority of cosmic rays that bombard the earth. Solar cosmic rays originate from the sun and make up a small amount of the cosmic rays seen around the earth. [Refs. 9, 10, 11, 12]

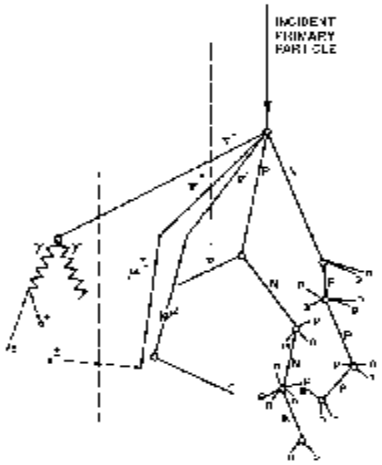

Figure 2.7. Cosmic Ray Shower [From Ref. 12.]

2. Solar Plasma

A second type of radiation that exists in space is called solar plasma. Plasma is a low-density mass similar to a gas, but consists of charged particles, mostly electrons and protons. [Ref. 13] Solar plasma streams radially into space at high speed reaching speeds of 450 km/s or more. [Ref. 9] This stream of solar plasma combines with the Sun's magnetic field to form solar wind and continuously bombards the earth with particle radiation. The earth is protected from this particle radiation by its magnetosphere. [Refs. 9, 14]

The core of the Earth is composed of molten iron-nickel, which causes it to act as a giant dipole bar magnet. The magnetic field radiates outwards from the Earth from north and looping to the to south. [Refs. 9, 13] The area of this magnetic field is called magnetosphere. Because solar wind carries a magnetic field, it interacts with the magnetosphere and is diverted from the earth surface in much the same way that water in a stream is diverted around rocks in its path. [Ref. 13] This is evident in the extreme northern and southern latitudes. The Aurora Borealis or Northern Lights is caused by the interaction of the solar wind with earth's magnetosphere. [Ref. 13] Figure 2.8 depicts the solar winds interacting with the earth's magnetosphere. The solar wind acting on the earth's magnetosphere causes it to become distorted. The magnetosphere diverts most of the solar plasma but some charged particles do manage to become trapped inside the earth's magnetosphere in two regions called the Van Allen belts. [Refs. 9, 13]

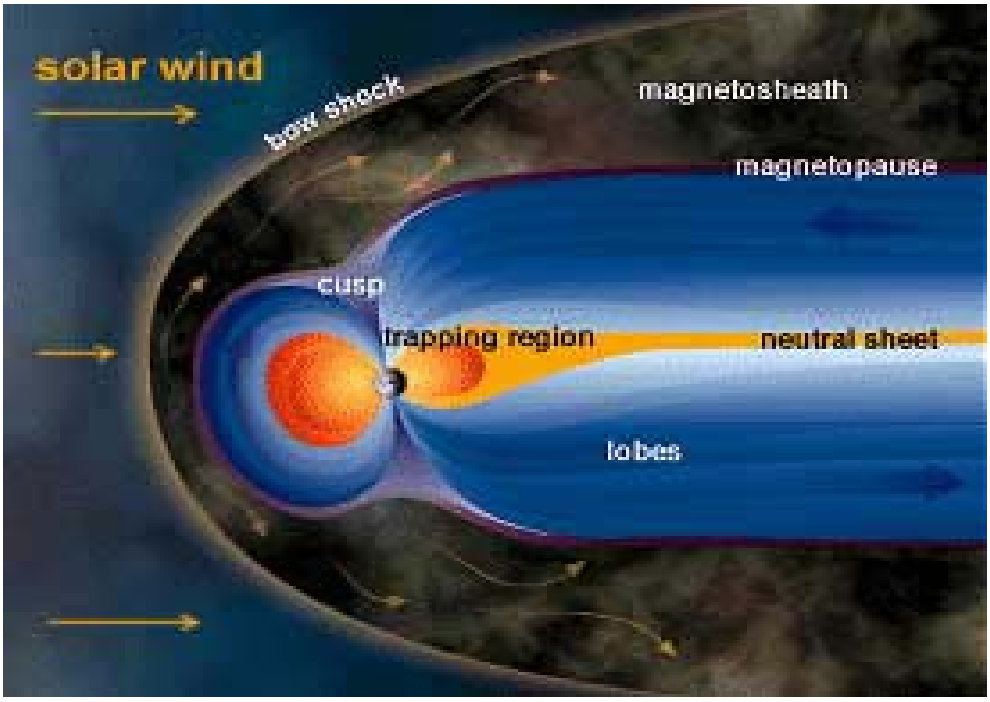

Figure 2.8. Solar Wind and Magnetosphere [From Ref. 13.]

3. Van Allen Belts

The two Van Allen radiation belts contain charged particles trapped in the Earth's magnetic field. Figure 2.9 depicts the inner and outer rings of the Van Allen belts that surround the earth. [Ref. 12] The primary component of the inner belt is high-energy protons, produced when cosmic rays shoot particles out of the upper atmosphere. The outer belt consists primarily with high-energy electrons which are produced by cosmic rays and magnetospheric acceleration processes. [Ref. 14] During steady-state conditions in the magnetosphere, particles neither enter nor escape these trapped orbits. During magnetospheric disturbances, however, accelerated particles may enter and leave the Van Allen belts. [Refs. 12, 14]

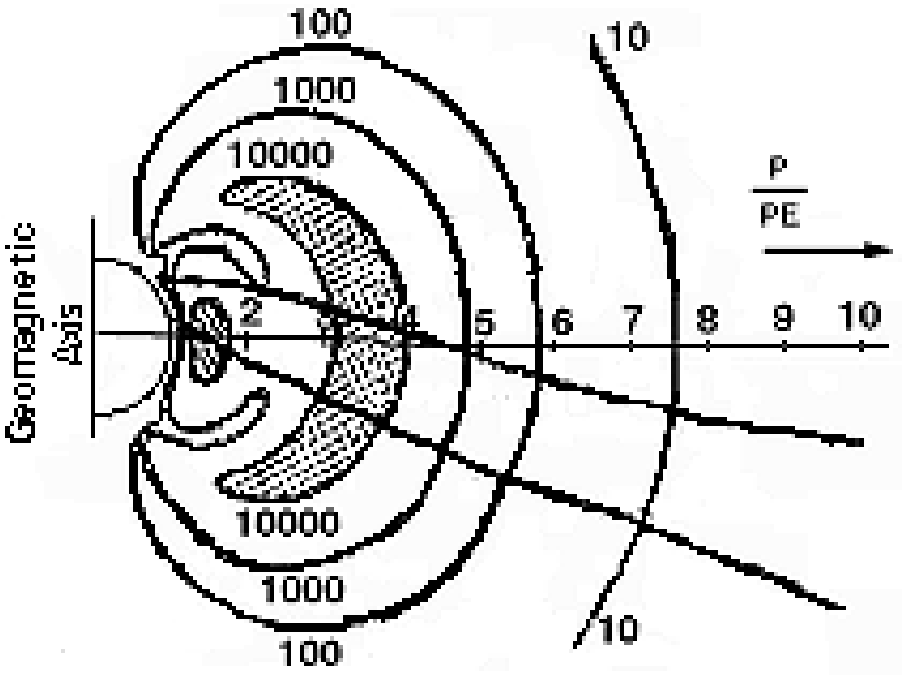

Figure 2.9. Van Allen Belts [From Ref. 12.]

The Van Allen Belts were discovered in 1958, when a Geiger counter mounted onboard Explorer I, provided surprising evidence that the Earth is surrounded by intense particle radiation. [Ref. 14] Additional data was collected from subsequent missions and experiments and found that two huge zones of trapped electrons and protons encircle the Earth. These belts lie approximately within the plasma sphere and are named after their discoverer, the Van Allen belts. [Ref. 14]

D. RADIATION EFFECTS

The purpose for studying the different types of radiation in space is to ascertain the effects of radiation on silicon devices. The two major effects of radiation are ionization and displacement damage.

1. Ionization Damage

Ionization damage takes place when the outermost valance shell electron is stripped away from the atom by collision with a charged particle or a photon. [Ref. 3] If one or more obital electrons are stripped from the atom, it is left with a net positive charge and is referred to as a positive ion. [Refs. 6, 7] The freed electrons are referred to as negative ions, and the two are referred to as the ion pair. In semiconductor devices

ionization results in the creation of electron-hole pairs. [Refs. 15, 16] The operation of these semiconductor devices depends on the doping level of the substrate. The creation of electron-hole pairs changes the level of doping of the substrate and can change the performance of the device. [Refs. 8, 15, 16]

2. Displacement Damage Effects

In silicon devices displacement damage takes place when an atom is dislodged or displaced from its lattice structure by the momentum of a particle moving with high energy. [Refs. 15, 16] This type of damage is usually caused by neutron radiation. The damage caused by the bomdarding neutrons dislodge the atoms in the semiconductor crystal creating an interstitial-vacancy pair known as a Frenkel defect. [Ref 16] These defects in the semiconductor lattice create resistivity changes within the crystal lattice by creating trapping centers for the minority carriers. [Ref. 8] This effect can cause an increase in the collector-base reverse current (I_{CBO}) which introduces leakage across the collector-base pn junction. [Refs. 15,16] This leakage across the collector-base pn junction results in a decrease of the current gain denoted as β in bipolar junction transistors. [Refs. 15, 16]

3. Transient Damage Effects

Transient damage effects refer to the transient or temporary changes in the electrical properties of the semiconductor device due to ionization of the substrate. [Refs. 15, 16] The ionization of the substrate results in the generation of electron- hole pairs in the device. In semiconductor devices with pn junctions such as an active biased transistor, the effect of ionizing radiation results in the increased flow of minority carriers across the junctions. This flow of minority carriers is called photocurrent. The effects of photocurrents across the pn junction result in latch-up and breakdown. These effects are discussed in more detail in the following chapter. [Refs. 15, 16]

4. Surface Damage Effects

Surface damage effects refer to the changes in the electrical behavior of a semiconductor device due to the collection and migration of charge in the silicon dioxide layer on the surface of a transistor. [Refs. 15, 16] Surface damage effect is caused by exposure to ionizing radiation and is called semi-permanent because its effects are temporary but can persists for years after radiation exposure. Again the effect of surface

damage results in an increase in the collector-base reverse current (I_{CBO}) which introduces leakage across the collecor-base pn junctions. This leakage across the collector-base pn junction results in a decrease in the β of the transistor. [Refs.15, 16] Table 2.1 summarizes the effects of radiation on semiconductor devices. [Ref. 15]

Application	Damage Effect	Radiation	Device Affected
Nuclear Weapons	Displacement	η only	Bipolar Transistors
	Transient	η and γ	All semiconductor devices
	Surface	η and γ	IGFETs
Nuclear Reactor	Displacement	η and γ	Bipolar Transistors
	Transient	……	No problem
	Surface	γ only	Bipolar Transistors and IGFETs
Van Allen Belts	Displacement	e and p	Solar Cells only
	Transient	……	No problem
	Surface	e and p	Bipolar Transistors and IGFETs
η-neutrons γ - gamma rays p - positrons e - electrons			

Table 2.1. Summary of Radiation Effects on Semiconductor Devices [From Ref. 15.]

5. Annealing

Annealing refers to the semiconductor's ability to repair itself after exposure to damaging radiation by the recombination of crystal vacancies and interstitials. [Ref. 16] This results in improvement of the lattice integrity of the semiconductor and ultimately the improved performance of the semiconductor device after being irradiated. [Ref. 15] In most cases, atoms displaced by radiation are not stable at room temperature and as a result of thermal motion will anneal. [Ref. 8] In some cases the displaced atoms can form bonds with the impurities in the lattice which are stable at room temperature and will not anneal. [Ref. 8] The formation of stable impurity defects in semiconductor devices that act as trapping centers can ultimately lead to degradation in device performance. [Refs. 8, 15, 16]

The effects of radiation in semiconductor devices described in this chapter play key roles in this study. To better understand these effects it is important to understand the types of semiconductor devices that are being used and their operating characteristics. The following chapter will provide an introduction to the basic components such as the capacitor and Bipolar Junction Transistor (BJT), which are used to construct various types of Operational Amplifiers (OPAMPs). The effects of radiation on the performance of these components will ultimately affect the performance of the OPAMPs for this study.

III. SEMICONDUCTOR DEVICES

The majority of electronic components used in satellites and other spacecraft are of semiconductor devices. Of these semiconductor devices, the operational amplifier or op amp is the most versatile and the most commonly used. The most common building blocks for the op amp are the bipolar junction transistor (BJT) and the capacitor. BJTs can be used as amplifiers or switches. Because of the high gain-bandwidth product, the BJT is popularly used for many analog and digital circuits. The capacitor is primarily an energy storage device, but in an internally compensated op amp it is important for the stability of the op amp. This chapter will discuss the operational characteristics of the BJT and the capacitor and discuss the effects of total dose radiation on the performance of these devices.

A. BIPOLAR JUNCTION TRANSISTORS

The BJT is essentially constructed by joining two pn junctions back to back. These two junctions are called the emitter-base junction (EBJ) and the collector-base junction (CBJ). [Ref. 4] When joined the junctions form three regions called the emitter region, the base region and the collector region. The three regions of the BJT can be arranged to form a PNP or an NPN transistor. The p-type region is constructed using silicon that is doped to provide an overall positively charged material with holes as the majority of the charge carriers. The silicon used for the n-type region is doped to provide negatively charged electrons as the majority charge carriers. [Ref. 4] The PNP and NPN BJT are duals of each other. The PNP has a p-type region emitter, an n-type region base, and a p-type region collector. The NPN has an n-type region emitter, a p-type region base, and an n-type region collector. [Ref. 4] Both types work exactly the same except the biasing voltages, the majority carriers, and the current directions are reversed. For a BJT to be used as an amplifier it must be biased to operate in the active mode. [Ref. 4] In an effort to avoid redundancy in discussing the operation of both types of BJTs, the PNP transistor will be the focus of discussion. The BJT can be biased to operate in three different modes: cutoff, saturation, and active. Table 3.1 lists the biasing requirements for each mode. [Ref. 4]

BJT Modes of Operation		
Mode	EBJ biased	CBJ biased
Cutoff	Reverse	Reverse
Active	Forward	Reverse
Saturation	Forward	Forward

Table 3.1. BJT Modes of Operation [From Ref. 4]

The cutoff and saturation modes are used for switching applications such as for logic circuits. The active mode allows the transistor to operate as an amplifier. [Ref. 4] Figure 3.1 provides an example of a PNP type BJT biased in active mode. The figure depicts the current flows though the transistor.

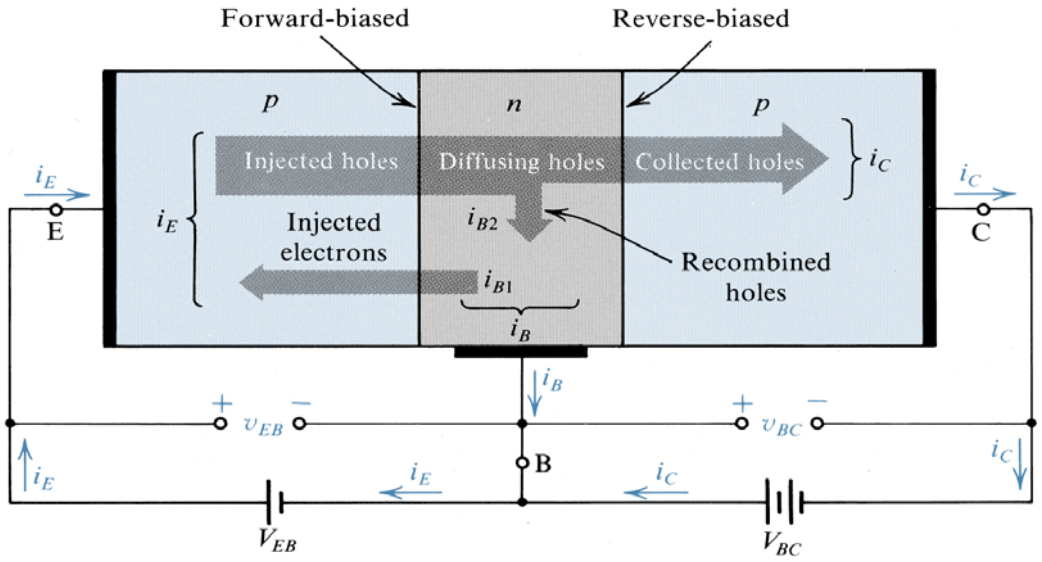

Figure 3.1. Current Flow of an Active Biased PNP BJT [From Ref. 4.]

1. Emitter Current

By forward biasing the EBJ, the voltage V_{BE} causes the positive emitter region to have a higher potential than the negative base region. This produces current flow i_E through the emitter consisting of electrons transiting from the base to the emitter, and holes transiting from the emitter to the base. The doping of the p-type material of the

emitter is significantly higher than that of the thin slightly doped n-type material of the base. Because of this, the majority of current (i_E) will consist of holes injected from the emitter. The electrons injected from the base will bring about the base current. [Ref. 4]

2. Base Current

There are two components that make up the base current (i_B). The electrons that are injected from the base to the emitter produce the first component. As the holes injected from the emitter pass through the base region, some of the holes will recombine with the majority carriers in the base and be lost. These lost electrons must be replenished from the circuitry external to the transistor. This provides the second component of the base current. [Ref. 4] Because the base region is so thin and the doping is much lower than the emitter region, most of the holes will continue on through the base and into the collector region. [Ref. 4]

3. Collector Current

The reverse bias of the CBJ with voltage V_{BC} causes the positive collector region to have a lower potential than the negative base region. The negative potential at the collector causes the holes coming though the base to be swept across the collector region as the collector current (i_C). [Ref. 4]

4. Collector-Base Reverse Current

In addition to the currents mentioned above, there are small reverse currents produced by thermally generated minority carriers. These currents are usually very small but, the reverse current in the CBJ region denoted as I_{CBO}, contains a substantial leakage component that increases as temperatures increase. The I_{CBO} could double for every $10°$ C increase in temperature. [Ref. 4]

5. Current Gain

To understand the performance of the BJT transistor it is important to understand the parameters that allow it to operate as an amplifier. The most important parameter is the common-emitter current gain denoted as β (also known as h_{FE}). Since β is a gain parameter, a high value for β is desired. The value for β is determined by the width of the base region and the level of doping in relation to the base and emitter regions. [Ref. 4] β is also the ratio of the collector current to base current,

$$\beta = i_C / i_B . \tag{3.1}$$

The value for β is usually in the range of 100 to 200 but can be higher for some special devices. [Ref. 4] Another important parameter is common-base current gain denoted as α. α is the ratio of the collector current to emitter current and is expressed by

$$\alpha = i_C / i_E . \tag{3.2}$$

The values of α and β are related to one another by the following equation:

$$\alpha = \frac{\beta}{\beta + 1} . \tag{3.3}$$

These parameters are used to determine the current values for the BJT. The following equations represent the relationship with the three transistor currents with the current gain parameters, [Ref. 4]

$$i_B = \frac{i_C}{\beta}, \tag{3.4}$$

$$i_E = \frac{\beta + 1}{\beta} i_C , \tag{3.5}$$

$$i_C = \alpha i_E , \tag{3.6}$$

and

$$i_E = i_C + i_B . \tag{3.7}$$

6. Radiation Effects on the BJT

The primary effect of total radiation dose is an increase in the leakage current (I_{CBO}) across the collector-base pn junction, which results in a decrease in current gain (β). [Ref. 15] The degradation of β is the most important parameter affected by radiation. [Ref. 16] Research conducted by Donald Brittain [Ref. 17] at Naval Postgraduate School irradiated several transistors operating in circuits using the school's linear accelerator (LINAC). Figure 3.2 reveals that β decreased with the increase in total dose radia

tion. Figures 3.3 and 3.4 show that β continued to decrease with an increasing total rad dose. In the latter case, β decreased an average of 35% of its original value with a total rad dose of 160 Mrad (Si). [Ref. 17]

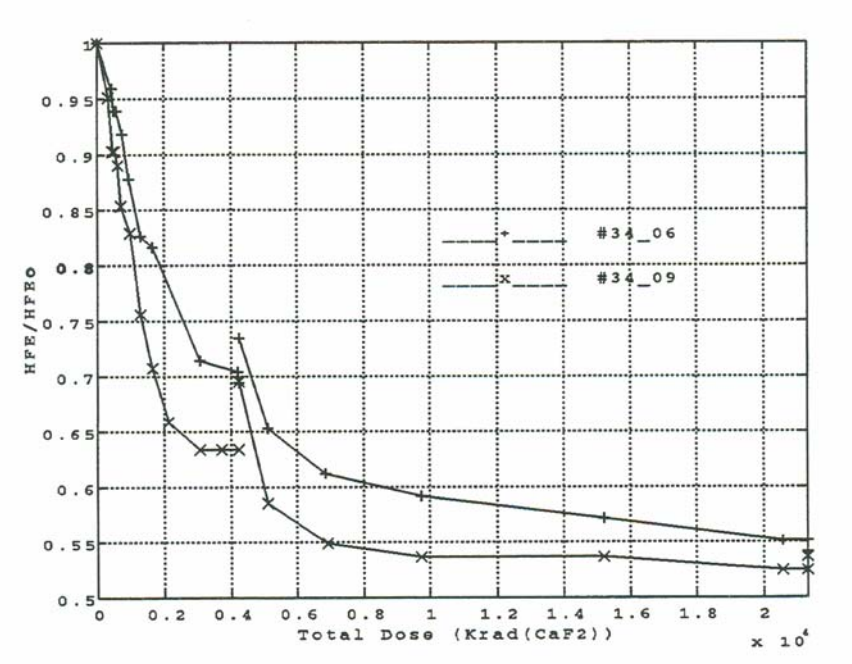

Figure 3.2. Effects of Total Rad Dose on β for Two Test Transistors [From Ref. 17.]

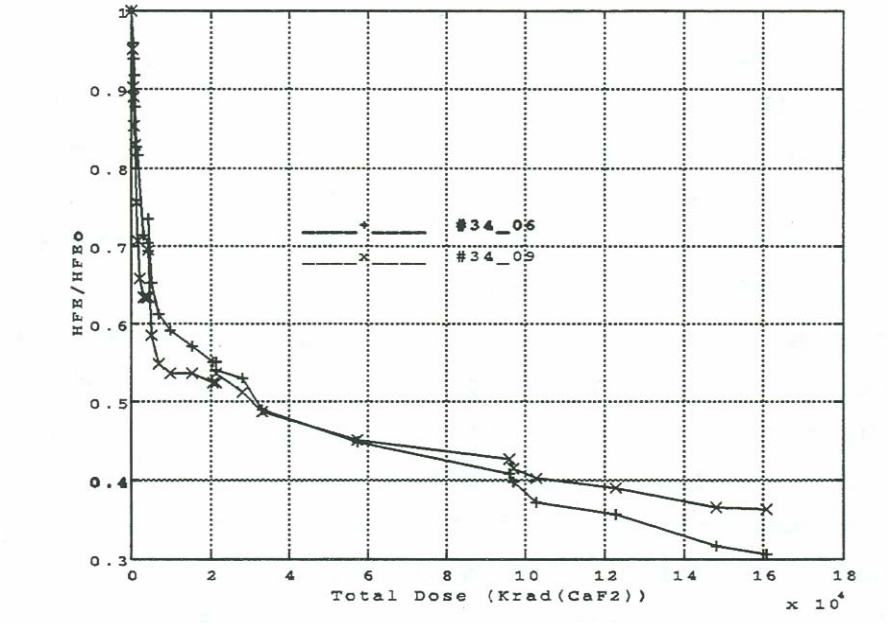

Figure 3.3. Effects of Total Rad Dose on β for Two Test Transistors [From Ref. 17.]

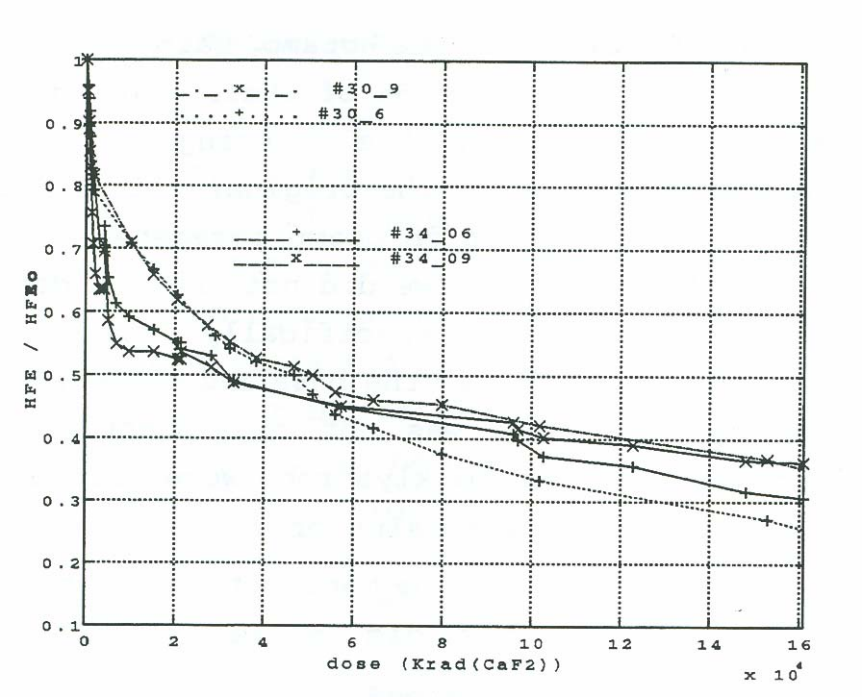

Figure 3.4. Effects of Total Rad Dose on β for Four Test Transistors [From Ref. 17.]

B. CAPACITOR

Capacitors are passive electronic devices that store energy in an electric field. The electric field is produced by applying a voltage to the device, which separates positive and negative charges on opposite plates. [Ref 18] The capacitor is constructed with two conducting plates separated by a dielectric. The capacitance is measured in farads and is directly proportional to the area of the conducting plates and inversely proportional to the distance between the plates. [Ref. 18] Capacitance is also directly proportional to the permittivity of the dielectric that separates the two plates. [Ref. 26] Figure 3.5 provides a general diagram of a metal oxide capacitor. [Ref 18]

1. Dielectric

The dielectric material is an insulator. Most dielectric materials are solid. Examples of dielectric materials include porcelain, mica, plastics and metal oxide. [Ref. 18] Other non-solid dielectric materials include distilled water, dry air or other gases such as nitrogen or helium. Two important properties of dielectric materials are the dielectric loss and the dielectric constant. [Ref. 18]

Dielectric loss refers to the proportion of stored energy that is lost as heat. The lower the dielectric loss, the more efficient the dielectric material and better the capacitor will be at storing energy. [Ref. 18]

The dielectric constant refers to the material's ability to concentrate the electrostatic lines of flux. [Ref. 18] Dielectric materials such as dry air or other gases have a low dielectric constant. Metal oxides have a very high dielectric constant. An advantage of dielectric material with a high dielectric constant is that it makes it possible to build rather large value capacitors with a small physical volume. [Ref. 18]

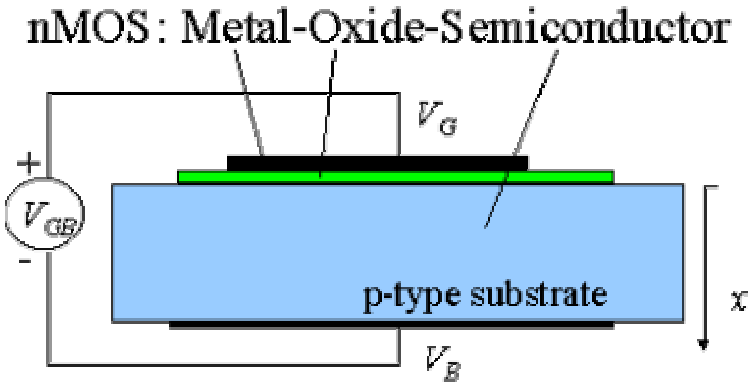

Figure 3.5. Metal Oxide Capacitor [From Ref. 26.]

C. RADIATION EFFECTS ON THE CAPACITOR

Capacitors are relatively sensitive to the effects of ionizing radiation. Ionizing radiation creates electron-hole pairs in the dielectric material, which increases the conductivity of the dielectric material. [Ref. 16] Two separate studies were conducted at Naval Postgraduate School that focused on the effects of radiation on capacitors.

One study was conducted by Stuart Abrahamson [Ref. 19] in which he investigated the effects of radiation on several parallel-plate metal oxide capacitors. His research focused on the performance of these capacitors placed in a low-pass filter after being irradiated with 26 MeV electrons from the school's linear accelerator (LINAC). His conclusions were that the 3-dB frequency of the filters dropped and that the electrical properties of the capacitors changed with radiation exposure. Afterwards the capacitors behaved like capacitors with increased capacitance values. [Ref. 19]

A second study was conducted by Duane Salsbury in 1996. [Ref. 20] The focus of his research was to investigate the effects of radiation on MOS VLSI capacitors. Two capacitors were used to construct two low-pass filters and were irradiated to a total rad dose of 2.66 MRad (Si). The schematic for the low pass filter used in his experiment is provided in Figure 3.6. The capacitance was measured by observing the value of the 3-dB frequency and then using the relationship

$$C = \left(2\pi R_1 f\right)^{-1} \tag{3.8}$$

to calculate the capacitance value. [Ref. 20] The variable f is the 3-dB frequency and R_1 is the 1 $\mathrm{M}\Omega$ resistor used in the circuit. [Refs. 4, 20]

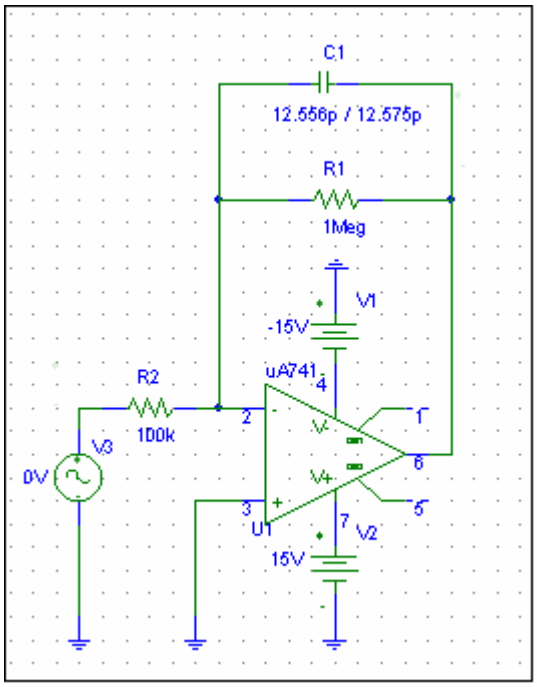

Figure 3.6. Low-Pass Filter [From PSPICE.]

From his experiments he concluded that the capacitance values did increase as a result of total dose radiation. Figure 3.7 provides the plotted results for the two capacitors tested. The graph reveals that the capacitance of both capacitors increased at an exponential rate.

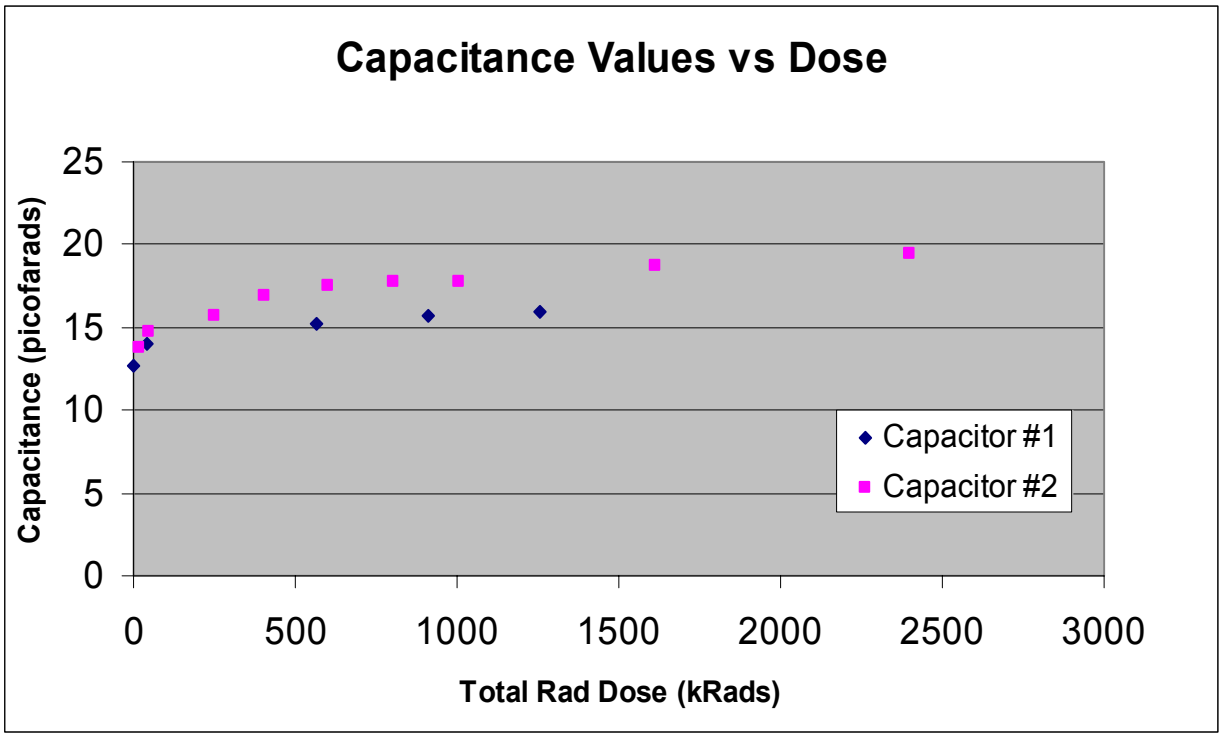

Figure 3.7. Capacitance vs. Total Rad Dose [From Ref. 20.]

The bipolar junction transistor and capacitor are the major building blocks for the operational amplifier. It is important to understand the operating characteristics of these components and the effects of radiation on these components to appreciate fully the operation of the op amp and its performance after total dose radiation. Chapter IV covers in detail the operational characteristics of the single op amp and composite op amp along with radiation effects on their performance.

THIS PAGE INTENTIONALLY LEFT BLANK

IV. SINGLE AND COMPOSITE OPERATIONAL AMPLIFIERS

The operational amplifier or op amp is one of the most useful circuits available to the engineer. The op amp as an integrated circuit (IC) is a versatile building block, which can be used to design several different circuits just by changing the values and configurations of the passive components external to the op amp IC. [Ref. 4] A special configuration places two or more op amps in tandem. This configuration is called the composite op amp and vastly improves the operational characteristics over the single op amp. [Refs. 3,5] Op amps can be constructed in several different ways. The most common types are constructed with BJTs, CMOS transistors or a combination of the two called a BiCMOS. This study will focus on the 741 op amp which is a BJT type internally compensated op amp. Figure 4.1 provides the circuit symbol for a 741 op amp. This section will discuss the operational characteristics of the single 741 op amp and the composite op amp constructed with two 741 op amps and the effects of total dose radiation on these circuits.

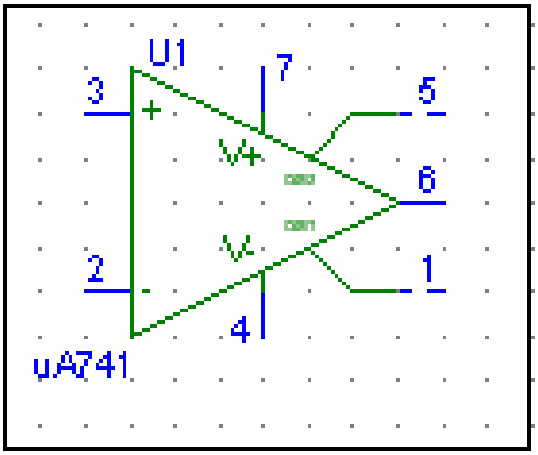

Figure 4.1. 741 Op Amp [From PSPICE.]

A. THE 741 OPERATIONAL AMPLIFIER

The 741 op amp is a high gain amplifier, which provides a high input impedance and relatively low output impedance. [Ref. 4] Figure 4.2 shows the schematic diagram of the 741 op amp. In analyzing the schematic, the 741 op amp can be divided into five sec

tions to describe its functional operation. The sections that make up the op amp are the bias circuit, the input stage, the second stage, the output stage, and the short-circuit protection circuitry. [Ref 4]

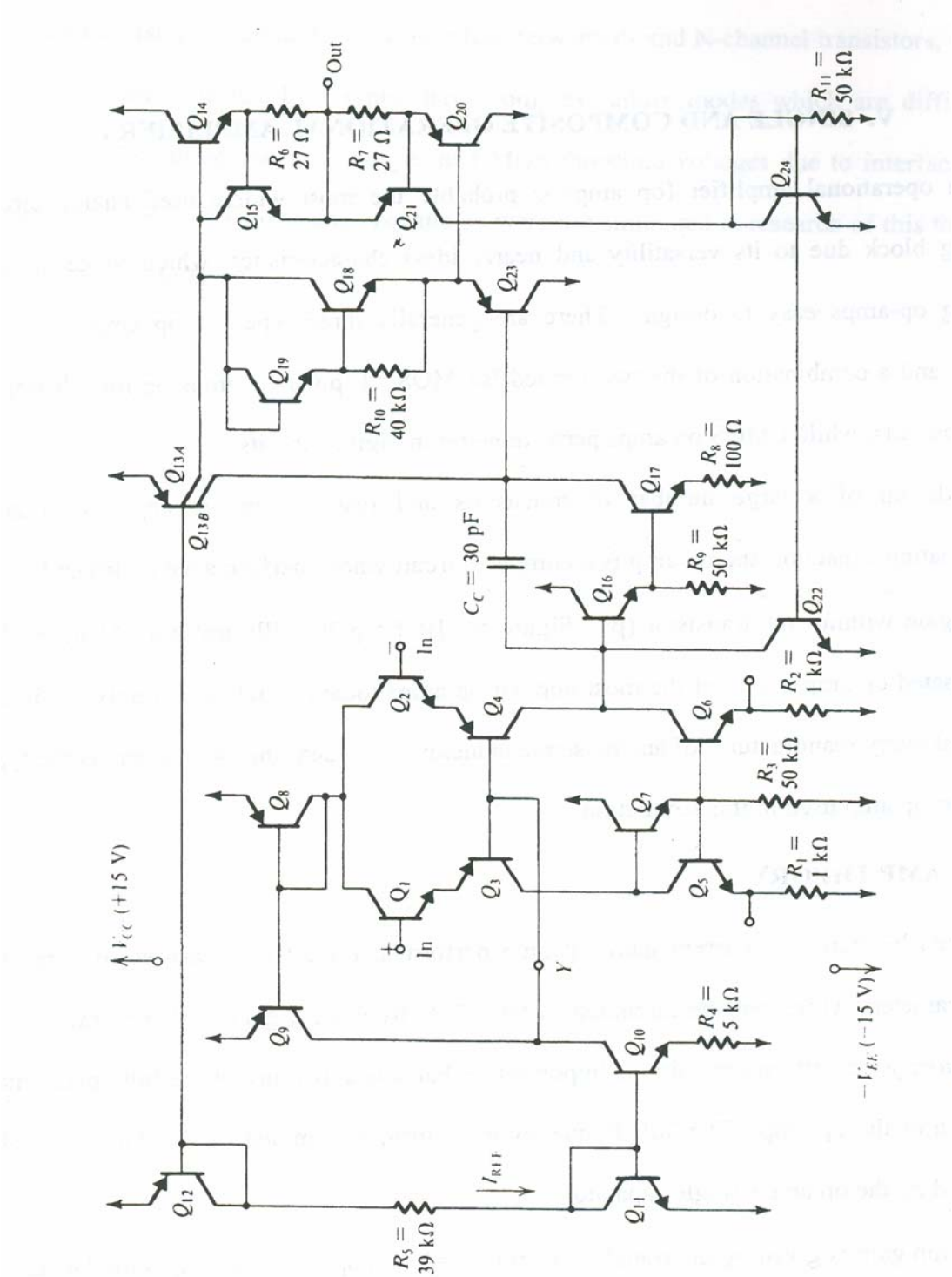

Figure 4.2. 741 Operational Amplifier [From Ref. 4.]

1. The Bias Circuit

The bias circuit provides the biasing reference current, I_{REF}, and the biasing currents for the rest of the circuit. The circuit consisting of the diode-connected transistors, Q_{11} and Q_{12}, and the resistor, R_5, are used to generate I_{REF}. [Ref. 4] The reference bias current I_{REF} can be approximated with the following equation

$$I_{REF} = \frac{V_{CC} - V_{BE12} - V_{BE11} - (-V_{EE})}{R_5}. \tag{4.1}$$

If $V_{CC} = V_{EE} = 15\text{ V}$ and $V_{BE11} = V_{BE12} \simeq 0.7\text{ V}$, then $I_{REF} = 0.73\text{ mA}$. [Ref. 4] The components Q_{10}, Q_{11} and R_4 form a Widlar current source which provides the biasing for the input stage via a current mirror formed by transistors Q_8 and Q_9. [Ref. 4] Transistors Q_{12} and Q_{13} form another current mirror. [Ref. 4] Transistor Q_{13} can be considered two transistors Q_{13A} and Q_{13B} with their base-emitter junctions connected in parallel. Q_{13A} provides biasing current for the components of the output stage and Q_{13B} provides biasing current for Q_{17} of the second stage. Transistors Q_{18} and Q_{19} are arranged to provide two V_{BE} drops for biasing Q_{14} and Q_{20} of the output stage. [Ref. 4]

2. The Input Stage

Transistors Q_1 though Q_7 form the input stage. Figure 4.3 provides the schematic diagram for the input stage of the op amp. Transistors Q_1 and Q_2 are a matched pair whose bases are the non-inverting and inverting inputs to the op amp. [Ref. 4] The two transistors are configured as emitter-followers, which provide the high input impedance for the op amp. This portion of the input stage provides a differential input to the emitters of Q_3 and Q_4. These two transistors are configured as common-base amplifiers, which provide a buffer for the input stage. [Ref. 4] Transistors Q_5, Q_6, and Q_7 along with resistors R_1, R_2, and R_3 form an active load circuit for the output of the input stage. [Ref. 4] This circuit provides a high-resistance load and converts the differential output from the cascaded common-collector common-base differential amplifier to a single-ended output for the input stage with no loss in gain or common mode rejection. [Ref. 4] The output is taken from the collector of Q_6 and is passed to the second stage. [Ref. 4]

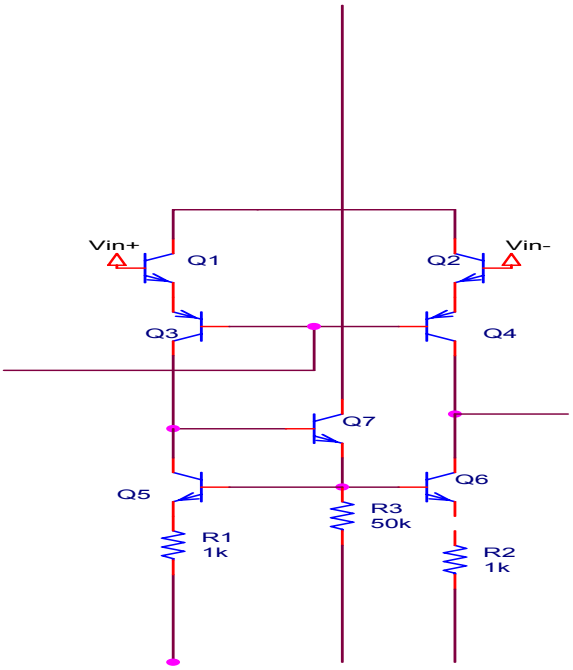

Figure 4.3. Input Stage [From Ref. 27.]

3. The Second Stage

The transistors Q_{16}, Q_{17}, and Q_{13B}, and resistors R_8 and R_9 make up the second stage. Figure 4.4 provides a schematic diagram of the second stage. [Ref. 4] The transistor Q_{16} is configured as an emitter follower amplifier so the second stage has high input impedance. [Ref. 4] Transistor Q_{17} forms a common emitter amplifier, which provides high voltage and current gain. [Ref.4] The capacitor C_C in the feedback loop with Q_{16} provides frequency compensation using the Miller compensation technique, which stabilizes the amplifier by introducing a dominant pole into the open-loop transfer function. [Ref. 4] The output of the second stage is taken from the collector of Q_{17}. [Ref. 4]

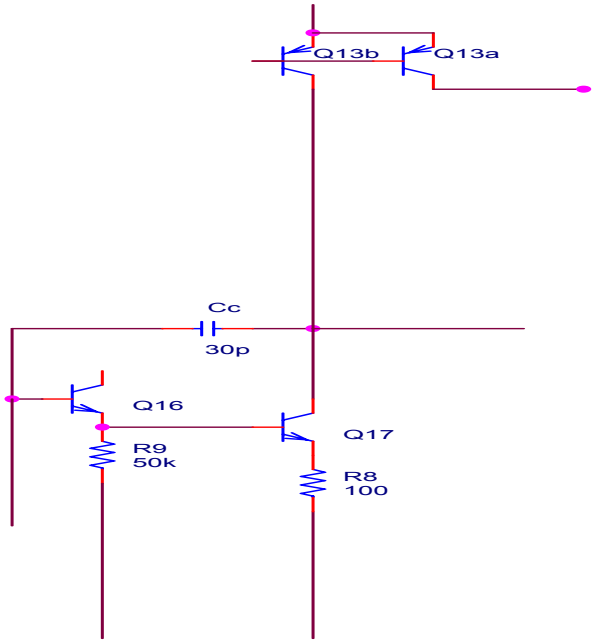

Figure 4.4. Second Stage [From Ref. 27.]

4. The Output Stage

The output stage consists of transistors Q_{14}, Q_{20}, Q_{18}, Q_{19} and Q_{13A}. Figure 4.5 provides a schematic diagram of the output stage. " Transistors Q_{18} and Q_{19} are fed by the current source Q_{13A} and bias the two output transistors Q_{14} and Q_{20}." [Ref. 4] The output stage provides low output resistance and can supply proportionally large load currents without dissipating excessive amounts of power throughout the op amp. [Ref. 4]

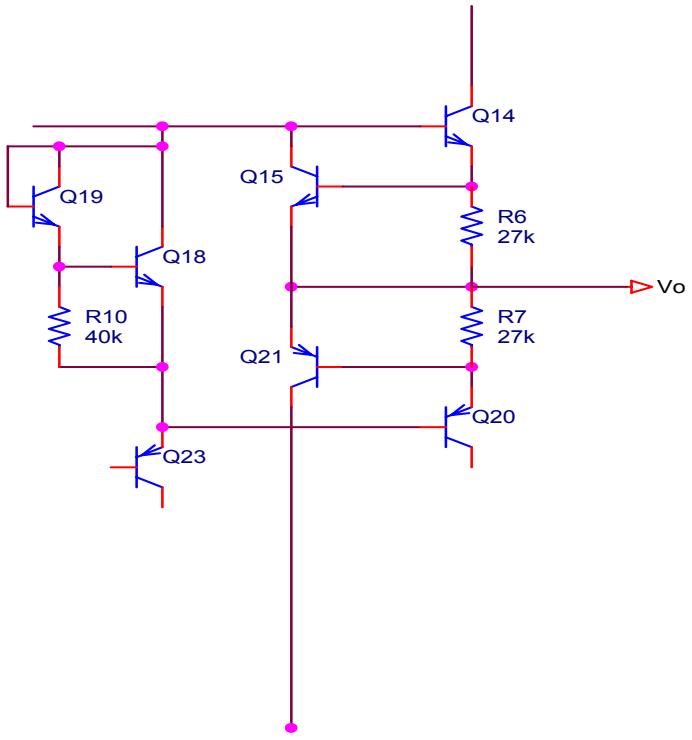

Figure 4.5. Output Stage [From Ref. 27.]

5. The Short Circuit Protection Circuit

The final section of the 741 is the short-circuit protection circuitry. Figure 4.6 provides a schematic diagram for a portion of this circuitry. This circuit is composed of transistors Q_{15}, Q_{21}, Q_{22} and Q_{24}, and resistors R_6, R_7 and R_{11}. [Ref. 4] These components make no contribution to the performance of the op amp. [Ref. 4] The transistors are normally off and will conduct only in the event that a large current is drawn from the output terminal. [Ref. 4]

Figure 4.6. Short Circuit Protection [From Ref. 27.]

B. THE COMPOSITE OPERATIONAL AMPLIFIER

The composite op amp was developed by Sherif Michael and Wasfy Mikhael in 1981 in an effort to extend the operational bandwidth and improve performance over the single op amp. [Refs. 3, 5, 23] Composite op amps are constructed by placing two or more single op amps in tandem joined by a simple circuit, which allows the entire group of op amps to perform as a single op amp with improved performance characteristics. [Ref. 5] Composite op amps are designated CNOA where *N* represents the number of op amps in the circuit. [Ref. 5]

C. COMPOSITE OP AMP THEORY

Initial investigations into the performance of CNOAs have been discussed in the literature [Refs. 3, 5, 22–24]. The procedure used for developing the CNOA derived by creating the necessary circuit topologies that met the performance criteria listed below.

- For all C2OAs, the denominator polynomial coefficients should satisfy the Routh-Horowitz criterion in that all coefficients have no change in sign. This is a necessary condition for stability. To desensitize the C2OA, none of the numerator or denominator coefficients should be realized through differences. [Refs. 3, 5]
- The external terminals of the C2OA should closely resemble that of the single op amp. [Refs. 3, 5]
- No closed loop zeros should appear in the right half of the s-plane in order to achieve minimum phase shifts. [Refs. 3, 5]
- The increased number of op amps should be justified by the improvement in frequency, gain, and phase performance over the single op amp. [Refs. 3, 5]

From the principles listed above, the C2OA's tolerance to mismatched active components and passive components make it appealing for use in circuits that must be designed to resist radiation degradation. [Refs. 3, 5] The degradation of op amp parameters such as gain, 3-dB frequency and slew rate will be less prominent with circuits that employ C2OAs than with circuits that utilize single op amps. [Refs. 3, 5] There are 136 different circuit combinations that have been experimented with. Of those different combinations the four listed in Figure 4.7 proved to be superior to the rest. [Refs. 3, 5]

Additional techniques were developed to further improve the operating parameters of the composite op amp. The Composite Multiple Operational Amplifiers (CNOAs) extend the operational bandwidth and improve the performance of the circuit at the expense of additional op amps. [Refs. 3, 5] A C3OA can be constructed by utilizing one of the four C2OA configurations and replacing one of the single op amps with another C2OA. Similarly, the C4OA can be constructed by replacing both of the single op amps with any one of the four C2OA configurations. [Refs. 3, 5] The research for this thesis concentrated on the C2OA type. The C2OA1 depicted in Figure 4.8 was the focus for this research and was used for simulations and comparisons.

D. RADIATION EFFECTS ON SINGLE AND COMPOSITE OP AMPS

Op amps are very susceptible to the effects of total dose radiation. Some of the main parameters affected are the gain, 3-dB frequency, gain bandwidth product (GBWP) and slew rate. [Refs. 3, 5, 16] In a previous research experiment conducted by Scott Sage at Naval Postgraduate School [Ref. 5], several circuits constructed with single and composite op amps were irradiated using the school's 110 MeV linear accelerator (LINAC). The op amps tested were the radiation hardened HS-5104RH and the non radiation hardened HA-5104. To measure the effects of total rad dose on these op amps, the parameters were measured while not allowing the irradiated op amps to anneal. [Refs. 3, 5] The non-radiation hardened HA-5104 used for this test was a general-purpose, low noise, high performance quad op amp. The HA-5104 has a slew rate of $3\,V/\mu s$ and 8-MHz gain bandwidth product. All of the tested op amps were manufactured from the same lot. [Refs. 3, 5, 21]

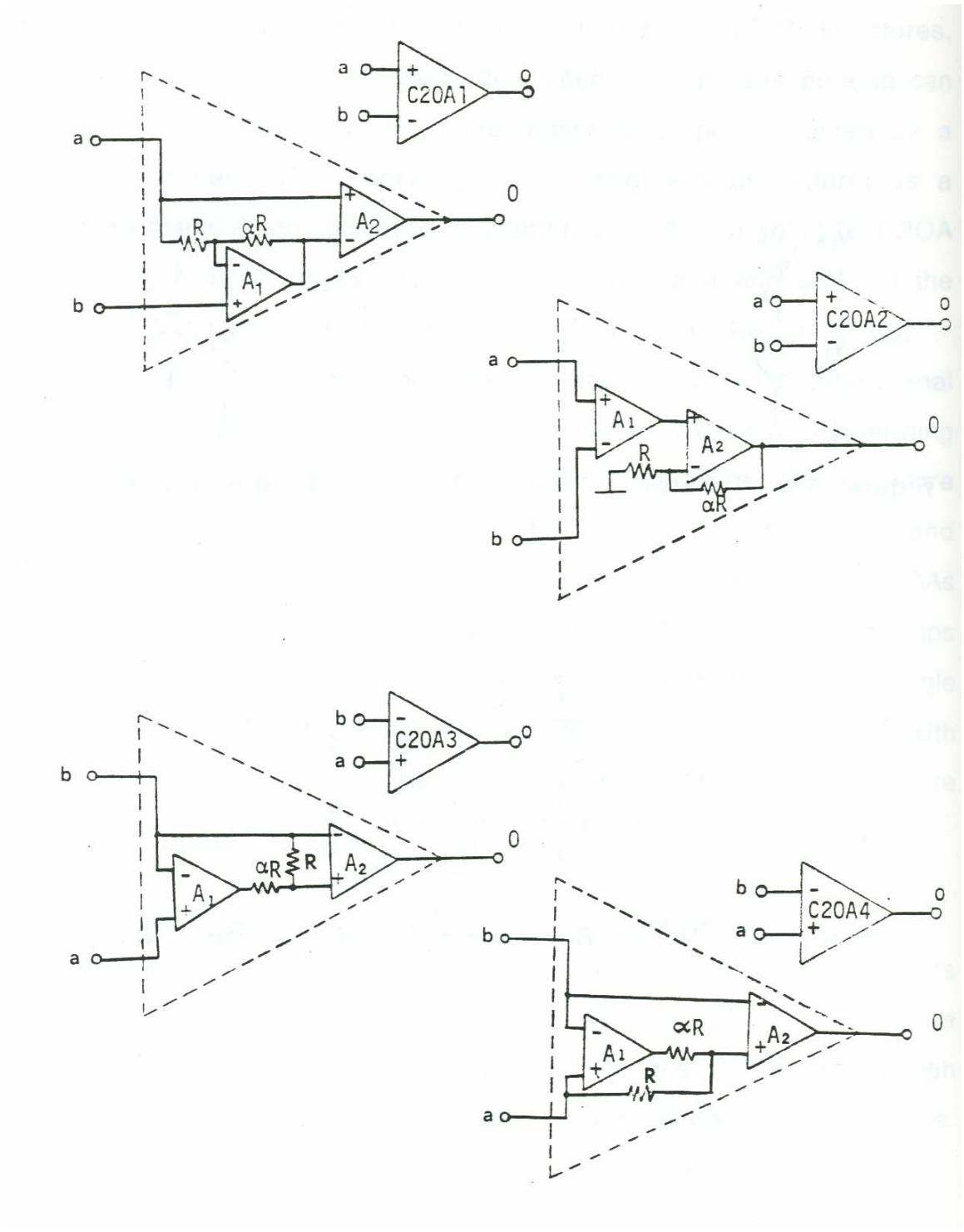

Figure 4.7. Superior C2OA Configurations [From Ref. 5.]

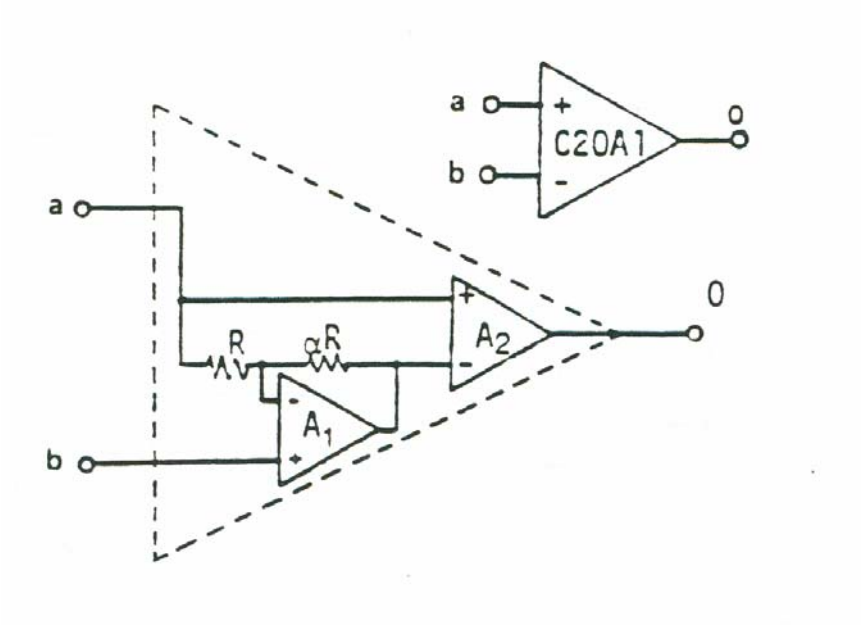

Figure 4.8. C2OA1 Composite Op Amp [From Ref. 5.]

The op amp circuits were tested in several different experiments. The op amps were configured as inverting amplifiers with a finite gain of 100. In each experiment, the circuits were irradiated to varying total rad doses up to 68 Mrad (Si). [Ref. 5] The results of two of these experiments are provided in Figures 4.9 though 4.13. The results of the first experiment are illustrated in Figures 4.9 and 4.10. The three non-radiation hardened op amps were irradiated up to 6 Mrad (Si). Circuits SOA1 and SOA2 are the single op amps and C2OA1 is the composite op amp. The graphs indicate that although all three circuits experienced degradation in performance, the performance of the composite op amp degraded a lesser amount and at a slower pace than the single op amps. This result is more pronounced in the second experiment with the rad-hardened op amps.

In the second experiment, the three rad-hardened op amps were irradiated up to 3 Mrad (Si). Again SOA1 and SOA2 are the single op amp circuits and C2OA1 is the composite op amp circuit. The results from the second experiment are provided in Figures 4.11 through 4.13. Again, the data reveals that the degradation in the percentage of gain and 3-dB frequency was less predominant in the composite op amp circuit than the single op amp circuit. In Figure 4.13, the actual 3-dB frequencies of the three circuits were plotted. Both the single and composite op amps experienced degradation but, again, the 3-dB frequency of the composite op amp remained far higher than that of the two single op

amps. Although the HS-5104RH and the HA-5104 op amps have different parameters than the 741 op amp, the effects of radiation should affect the components that make up these op amps in the same manner. By normalizing the results to obtain the percentage of change for each parameter, a reasonable baseline for conducting a comparative analysis is presented.

This chapter covered the operational characteristics of the single op amp and composite op amp and the effects of radiation on these two circuits. The data collected from these experiments conducted at Naval Postgraduate School were used as a baseline for modeling a PSPICE simulation and conducting a comparative analysis for this thesis. The following chapter discusses the set-up and description of that PSPICE simulation.

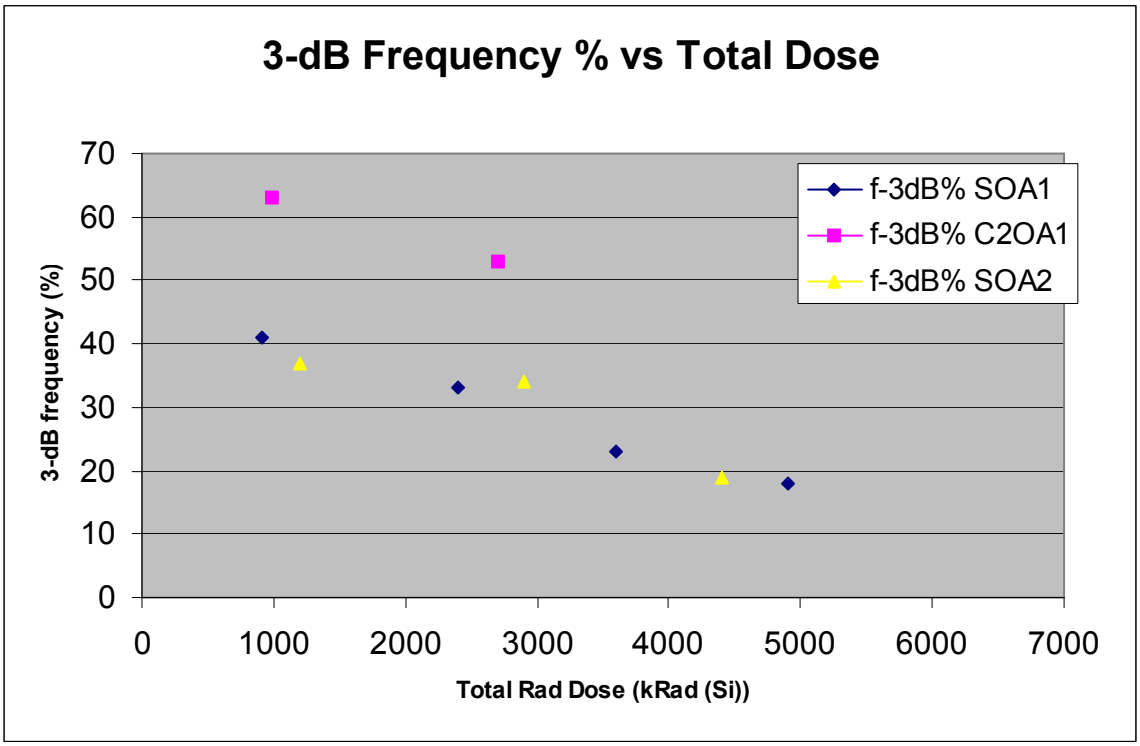

Figure 4.9. 3-dB Frequency % Change of Non-Radiation Hardened Single and Composite Op Amps [From Ref. 5.]

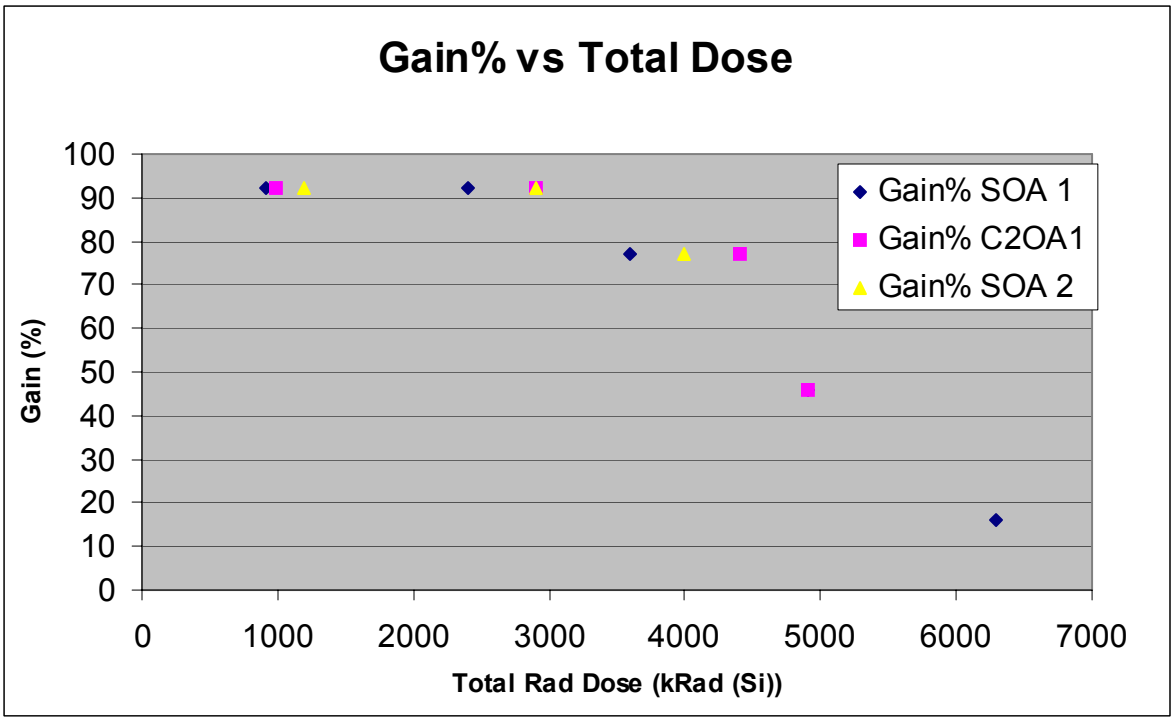

Figure 4.10. Gain % Change for Non-Radiation Hardened Single and Composite Op Amps [From Ref. 5.]

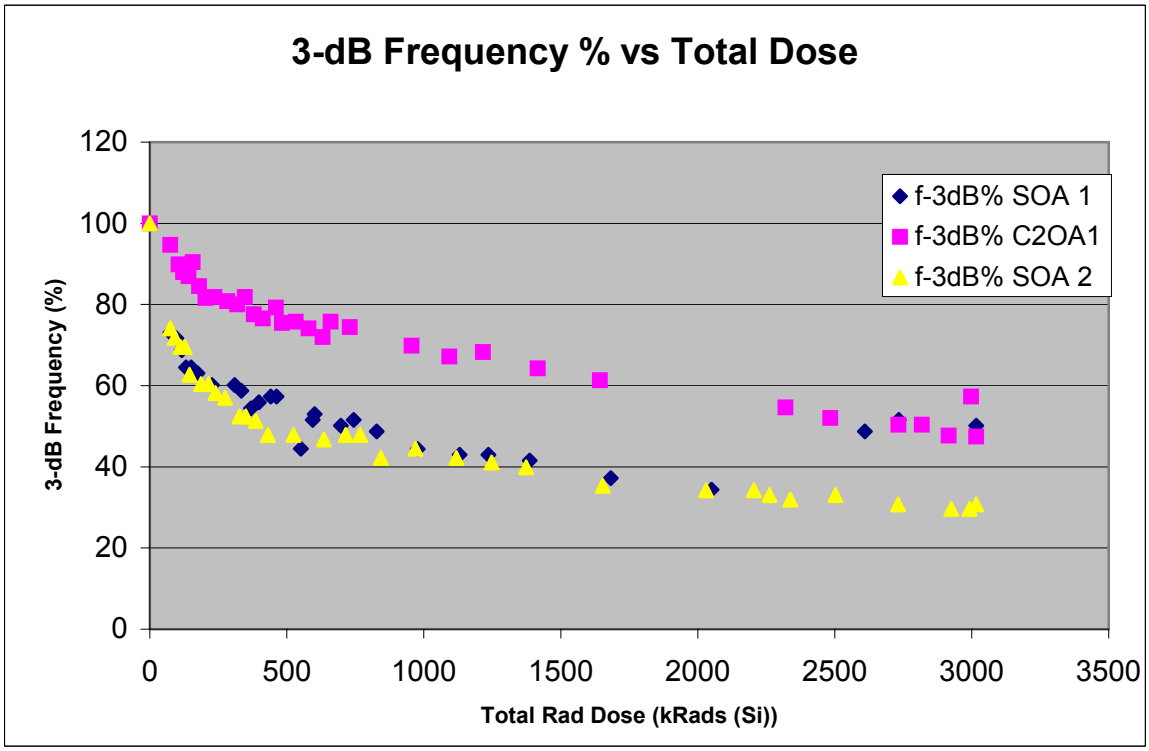

Figure 4.11. 3-dB Frequency % Change for Rad-Hardened Single and Composite Op Amps [From Ref. 5.]

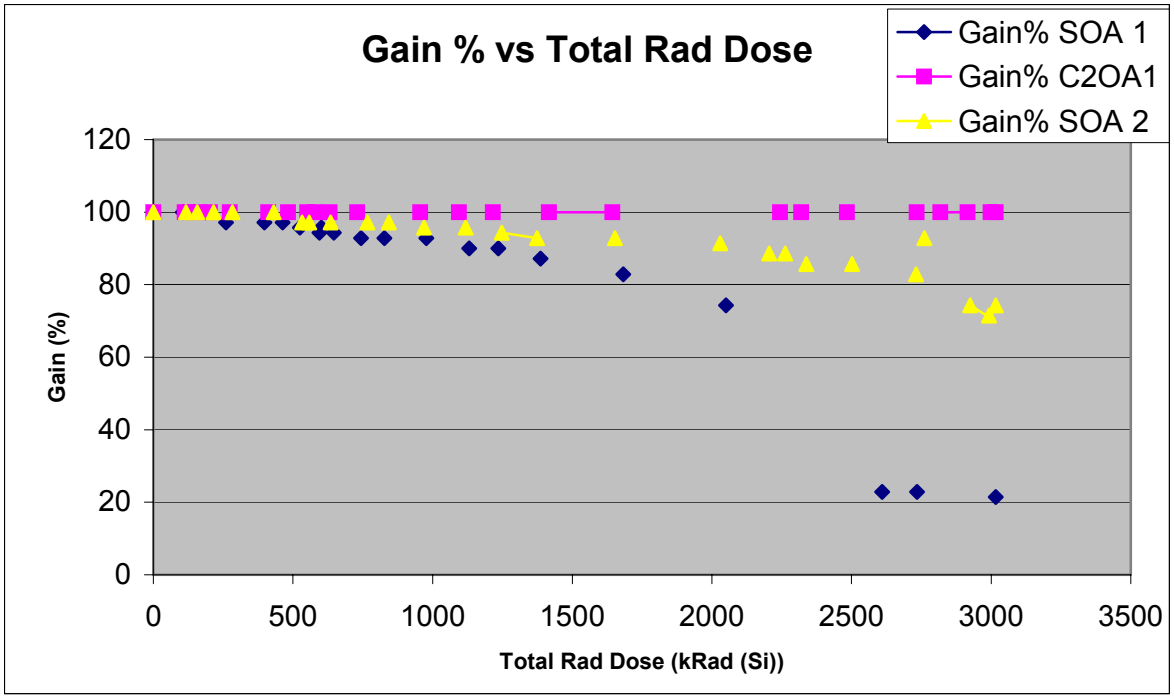

Figure 4.12. Gain % Change for Rad-Hardened Single and Composite OP Amps [From Ref. 5.]

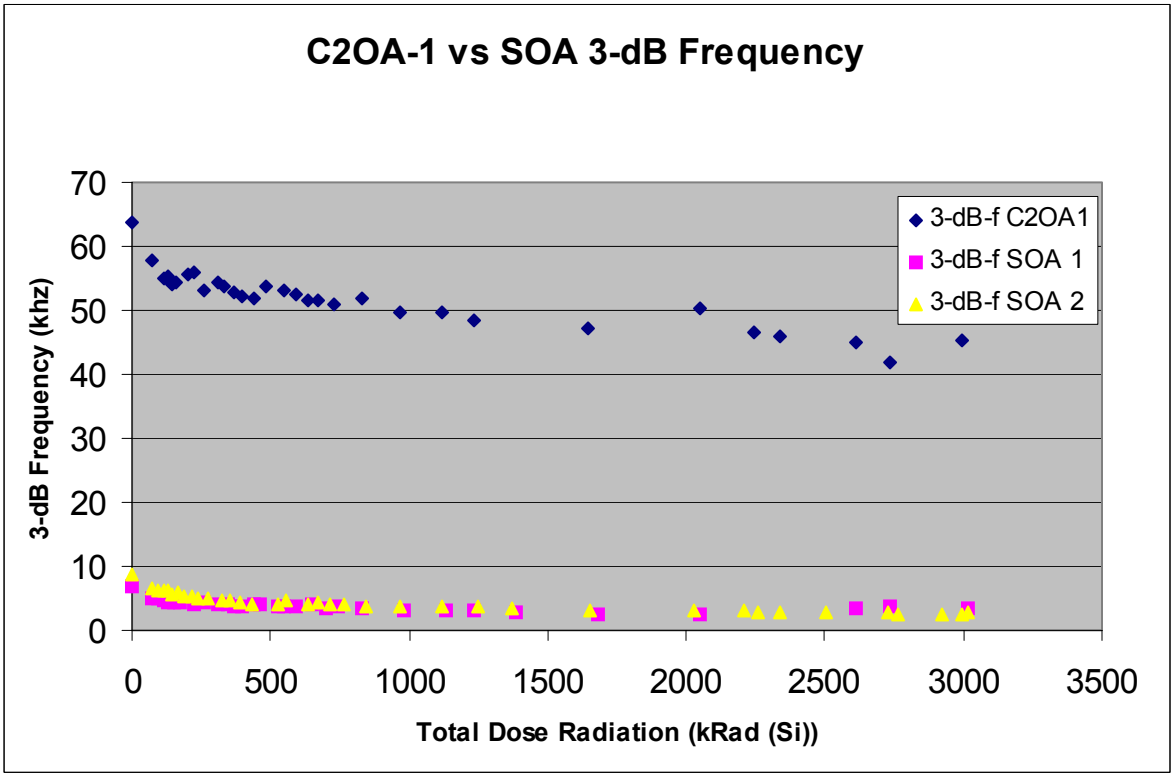

Figure 4.13. 3-dB Frequency of Rad-Hardened Single and Composite Op Amps [From Ref. 5.]

THIS PAGE INTENTIONALLY LEFT BLANK

V. SIMULATION PROCEDURE

A. BACKGROUND

This research is a continuation of an effort to simulate the effects of radiation on single and composite op amps using PSPICE. A previous endeavor was conducted by Rebecca Baczuk in 1994 at Naval Postgraduate School. [Ref. 3] Baczuk's approach was to find a correspondence between the transistor parameter variations and total dose radiation. The correspondence used for her simulations was the correlation that β decreased as total rad dose increased. Based on the results of experiments conducted at Naval Postgraduate School depicted in Figures 3.2 through 3.4, Baczuk plotted data, which presented normalized β values verses total dose radiation. This data is shown in Figure 5.1 and depicts the effects of total dose radiation on β out to 100 Mrads (Si). [Ref. 3]

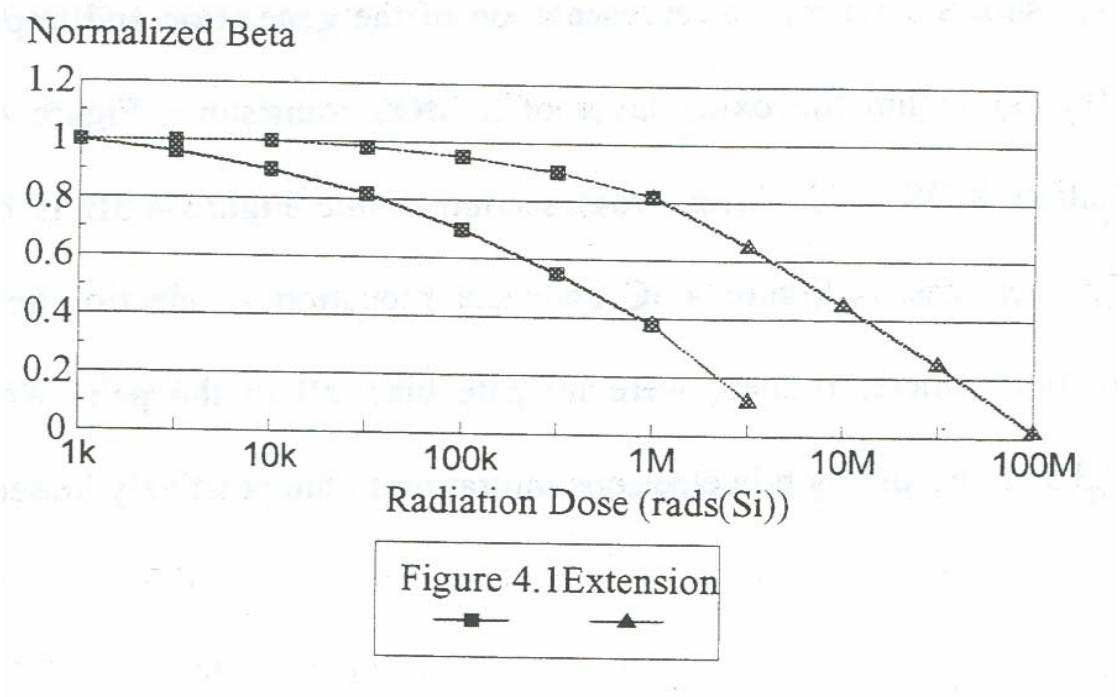

Figure 5.1. Normalized β Measurements vs. Total Rad Dose [From Ref. 3.]

Her next step was to construct in PSPICE a single op amp based on the 741 model depicted in Figure 4.2 and C2OA1 composite op amp depicted in Figure 4.7 using two 741 op amps. These two op amps were configured as a low-pass filter amplifier with a finite gain of 100. To simulate the effects of total dose radiation on these circuits, the β

parameter for each of the 25 transistors in each op amp was modified from their original value to reflect increasing total dose radiation. The percentages of β chosen were 100%, 50%, 10%, 5%, 4%, 3%, and 2.5%.

The simulations were run for both the single and composite op amps and the results are depicted in Figure 5.2 and 5.3, respectively. These results showed that the decrease in β did not significantly affect the gain until it was degraded to greater than 95% of its original value. In a comparison with the results of the radiation experiments conducted by Sage [Ref 5], the gain of the non-radiation hardened op amps proved to be greatly affected by the effects of radiation. For the radiation hardened op amps, the gain comparisons followed little closer, but other op amp parameters such as 3-dB frequency and GBWP did not follow with the simulated results. There was a need to investigate the effects of radiation on other op amp components and evaluate its overall effect on single and composite op amp performance.

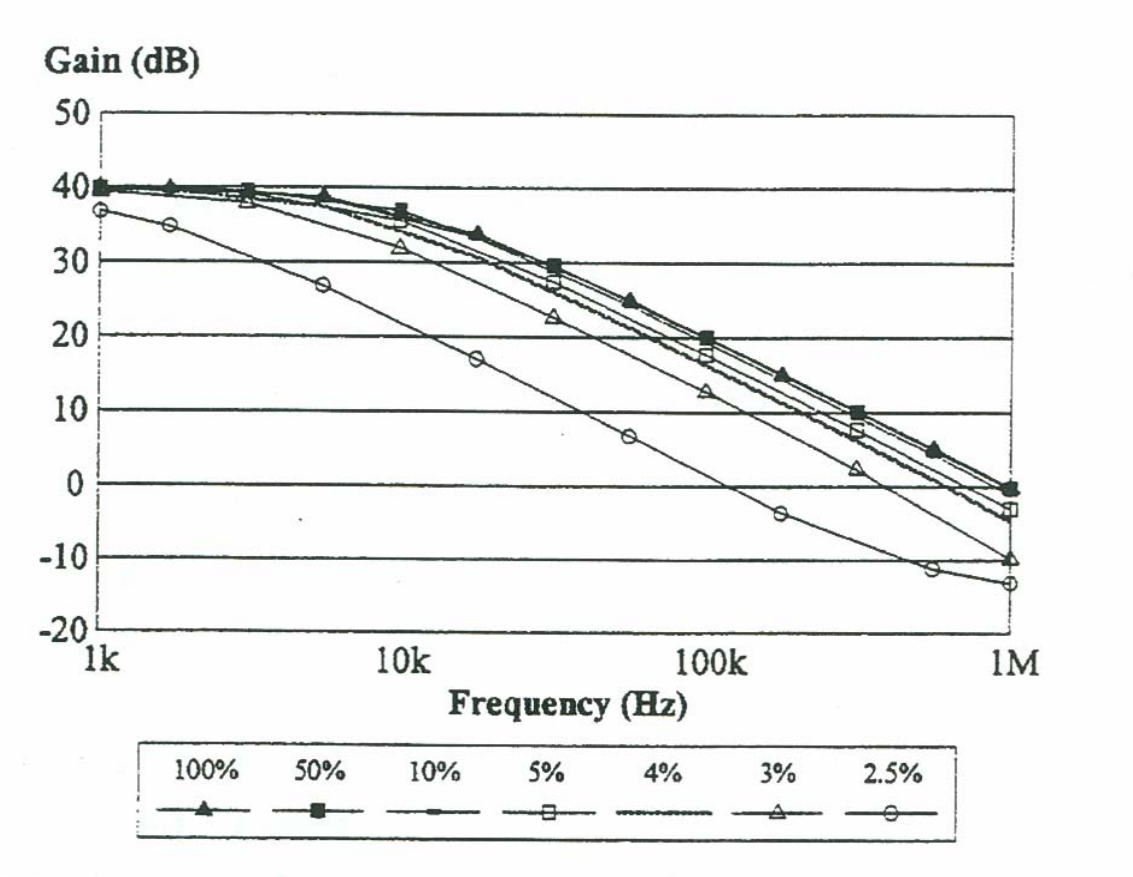

Figure 5.2. Results from Single Op Amp Simulations [From Ref. 3.]

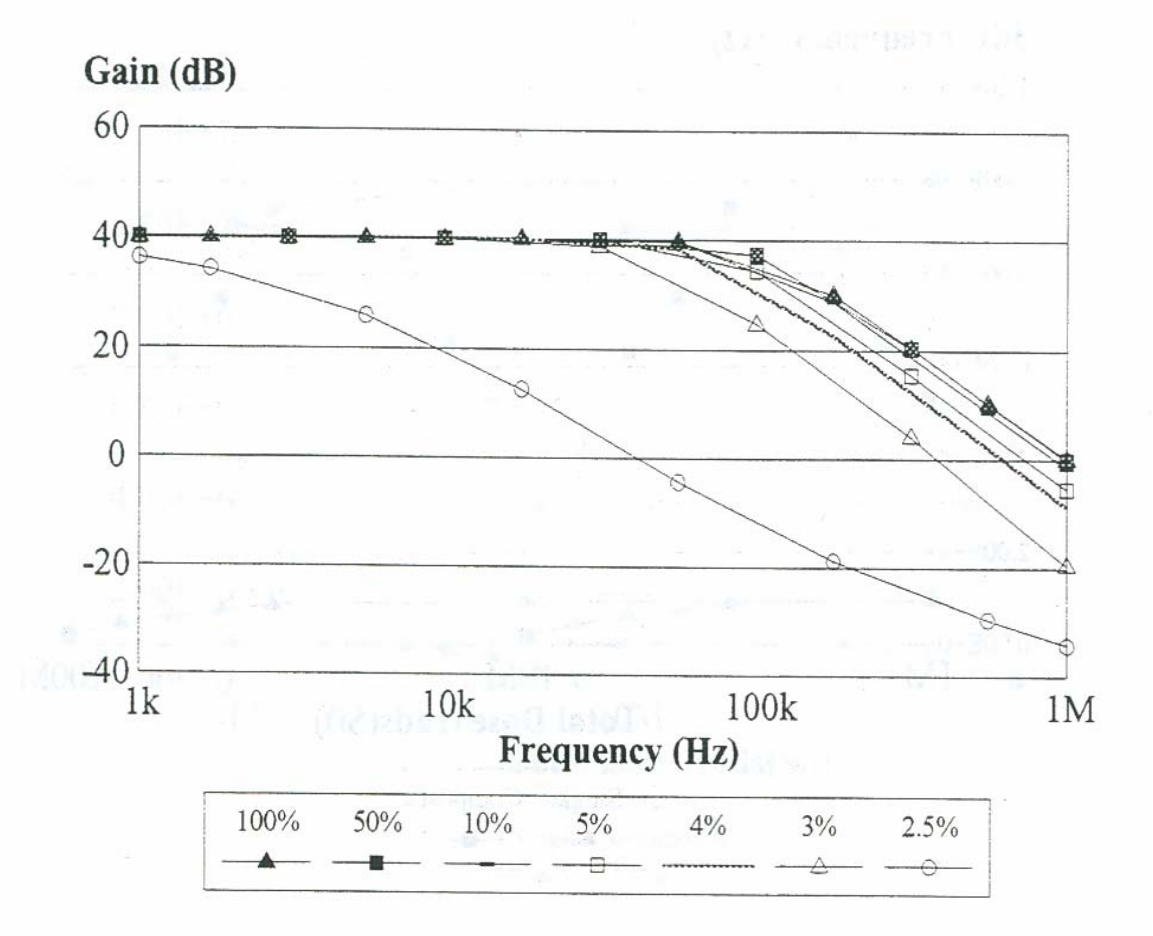

Figure 5.3. Results from C2OA1 Simulations [From Ref. 3.]

B. SIMULATION SET-UP

For the simulation conducted for this thesis, the approach taken was to first identify the major components of the single and composite op amps along with the effects of radiation on those components. Second was to correlate the parameter variations for those components to reflect total radiation dose. Finally, was to apply these parameter variations to the PSPICE model of the single and composite op amps and compare these results with the baseline data.

The single op amp was created in PSPICE modeled after the 741 op amp shown in Figure 4.2. The components used to construct the op amp were transistors, resistors and a capacitor. The transistors used to construct this circuit were the Q2N2222 (NPN) and the Q2N2605 (PNP). These transistors were used because these models allowed for the largest choice of parameter variations. To ensure that the 741 op amps in Figures 5.5

and 5.6 performed as close as possible to the previous simulations conducted by Rebecca Baczuk [Ref. 3], the same exact transistors parameters were entered for each transistor. Those parameters are listed in Table 5.1. [Ref. 3]

Mod	Type	BF	IS	CJE	CJC	CJS	Transistors
1	PNP	50	10F	.1F	1.05P	5.1P	Q3, Q4, Q8, Q9, Q12, Q21, Q23
2	NPN	200	10F	.65F	.36P	3.2P	Q1, Q2, Q5, Q6, Q7, Q10, Q11, Q15, Q16, Q17, Q18, Q19, Q22, Q24
3	PNP	50	2.5F	.1F	.3P	4.8P	Q13
4	PNP	50	7.5F	.1F	.9P	4.8P	Q25
5	NPN	200	10F	2.8F	1.55P	7.8P	Q14
6	PNP	50	10F	4.05F	2.8P	N/A	Q20

Table 5.1. Transistor Parameters [From Ref. 3.]

C. RADIATION SIMULATION

1. Transistor Correlation

To model the effects of radiation on the single and composite op amps with respect to the β of the transistors, historical and real data were used to correlate the effects of total dose radiation on the value of β for the transistors. Real data from actual experiments conducted at Naval Postgraduate School were correlated as well. Experiments conducted by Donald Brittain in 1995 [Ref. 17], irradiated several transistors and measured the β values. Figures 3.2 through 3.4 illustrate the results of experiments conducted over several days with a total radiation dose of 160 Mrad (Si). From the data available from these experiments, the value of β decreased on an average of 50% of its original value for a total radiation dose of 0.2 to 10 Mrad (Si). For this simulation the value of β was varied from 0% degradation to 50% corresponding to a total dose of 3 Mrad (Si).

2. Capacitor Correlation

The 741 op amp is internally compensated with a 30 pF capacitor for stabilization. To correlate the total dose effects of radiation on this capacitor, the experimental results obtained by Salsbury [Ref. 20] were used as a model for this simulation. Salsbury irradiated two VLSI MOS capacitor chips using the NPS LINAC. These capacitors were irradiated to a total dose of 2.399 Mrad (Si). The original and final capacitance values for these capacitors are listed in Table 5.2. Figure 3.7 depicts the charted results as the capacitors were irradiated from zero to 2.399 Mrad (Si). [Ref 20]

Capacitor	**Original Value**	**Final Value**
Chip #1	12.556 pF	19.41pF
Chip #2	12.575 pF	15.92 pF

Table 5.2. Capacitance Values Before and After 2.399 Mrad (Si) Dose [From Ref. 20.]

From the results shown in Figure 3.6 it can be seen that the increase in capacitance is exponential in both devices and they both tend to follow the same pattern. These results were used to create a model for simulating the total rad dose effect on the 30 pF compensating capacitor in the 741 op amp. The data results from capacitor #1 only had five data points and only represented a total rad dose of 1.258 Mrad (Si). The data results for capacitor #2 had significantly more data points and represented total rad dose out to 2.399 Mrad (Si) so the results from capacitor #2 were used as the model for this simulation. The simulation required data out to 3 Mrad (Si) so the results for capacitor #2 were extrapolated using a moving average forecast method. Since the plotted data was not linear, the percent of change was calculated from each data point to the next. These percentages of change were applied to the 30 pF compensating capacitor to correlate the effects of total rad dose on that capacitor. Figure 5.4 presents a comparison of the Salsbury's test capacitor #2 and the compensating capacitor values used for this simulation.

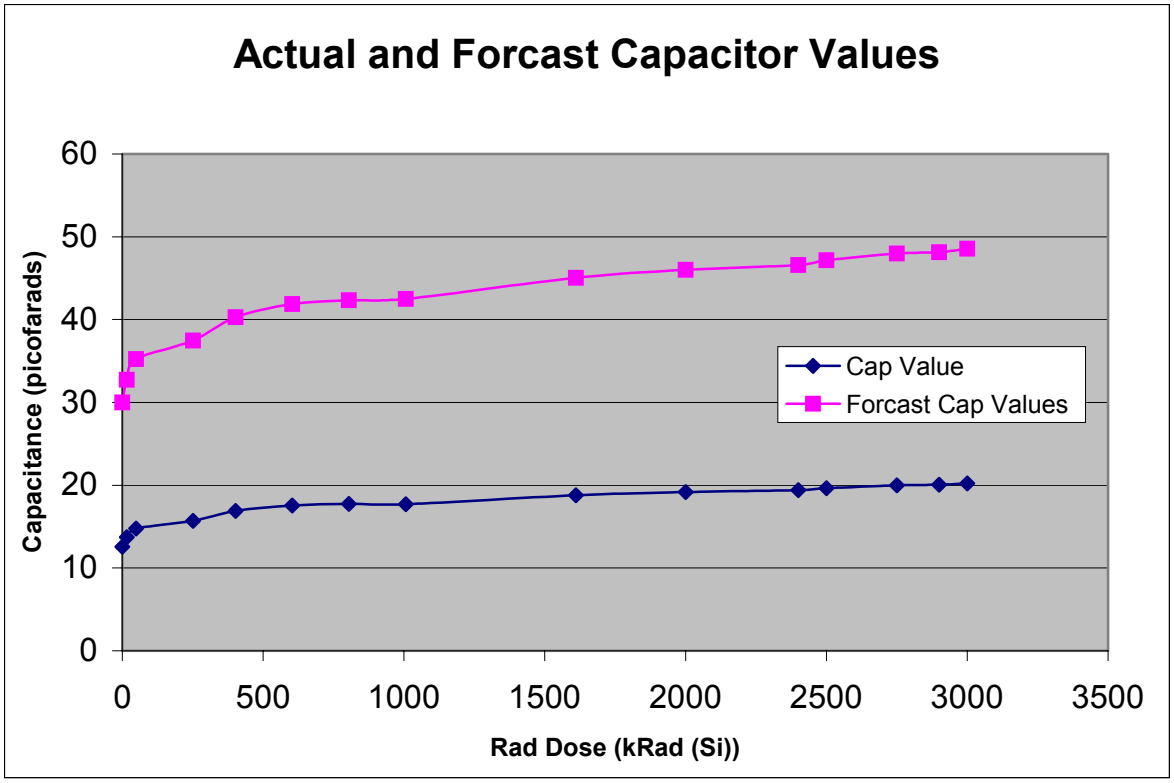

Figure 5.4. Comparison of the Actual Test Chip Values to the Predicted Compensating Capacitance Values Used for this Simulation.

D. SIMULATION PROCEDURE

For this simulation, the full version of MicroSim Release 8 Evaluation software (PSPICE) was used. The single and composite op amps were configured as low pass filter/amplifiers with a gain of 100. The configurations for the single and composite op amps are depicted in Figures 5.5 and 5.6, respectively. The input applied to the circuit was a 10-mV signal at 1kHz. The circuits were then simulated using the linear AC sweep and noise analysis function of PSPICE. The simulation was run 15 different times while varying the β values and capacitance values for each run to simulate an increasing total radiation dose. For each run the gain, 3-dB frequency and GBWP were collected for comparison to the actual results used as a baseline.

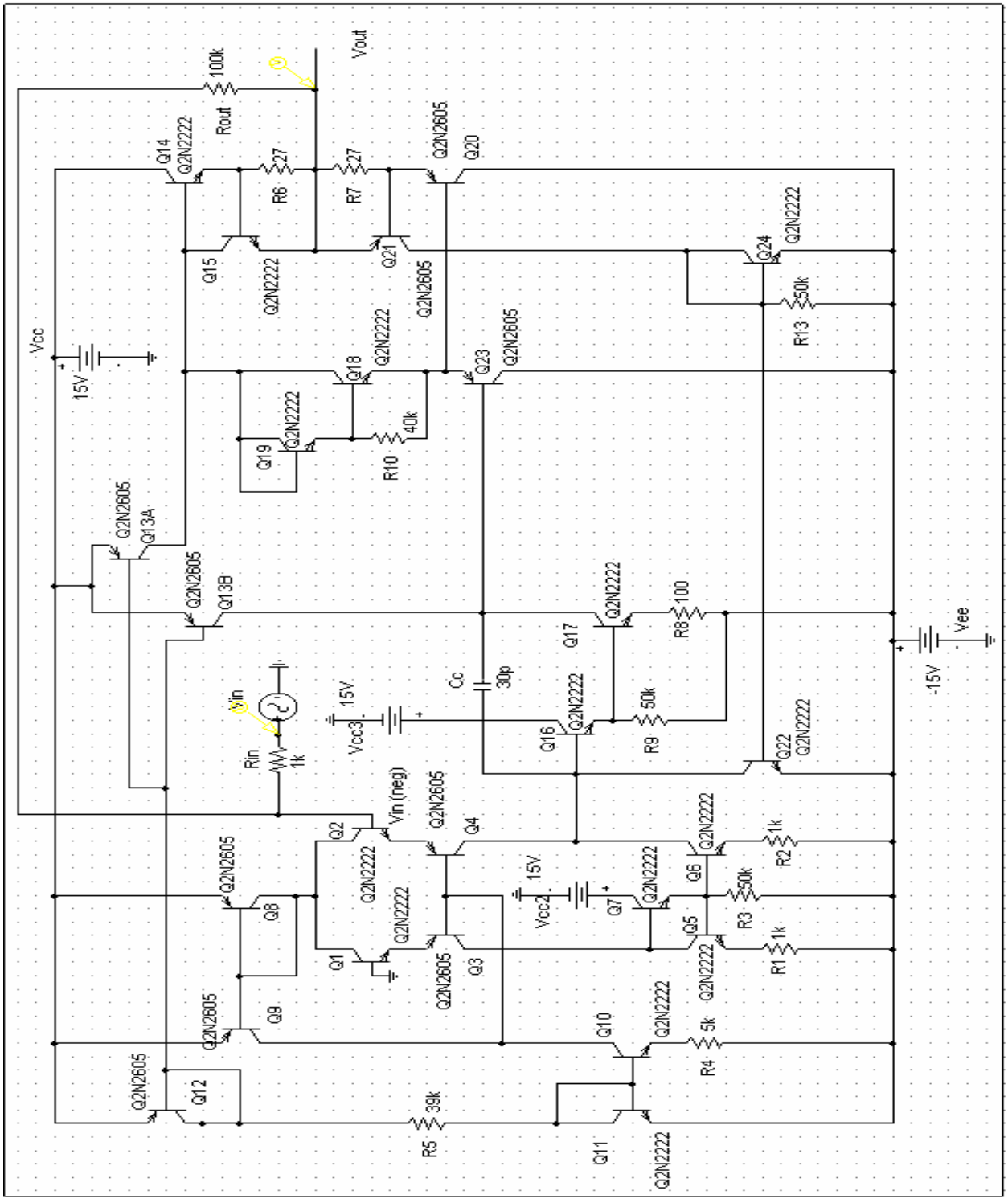

Figure 5.5. PSPICE Model of the Single Op Amp in the Finite Gain Amplifier Circuit [From PSPICE]

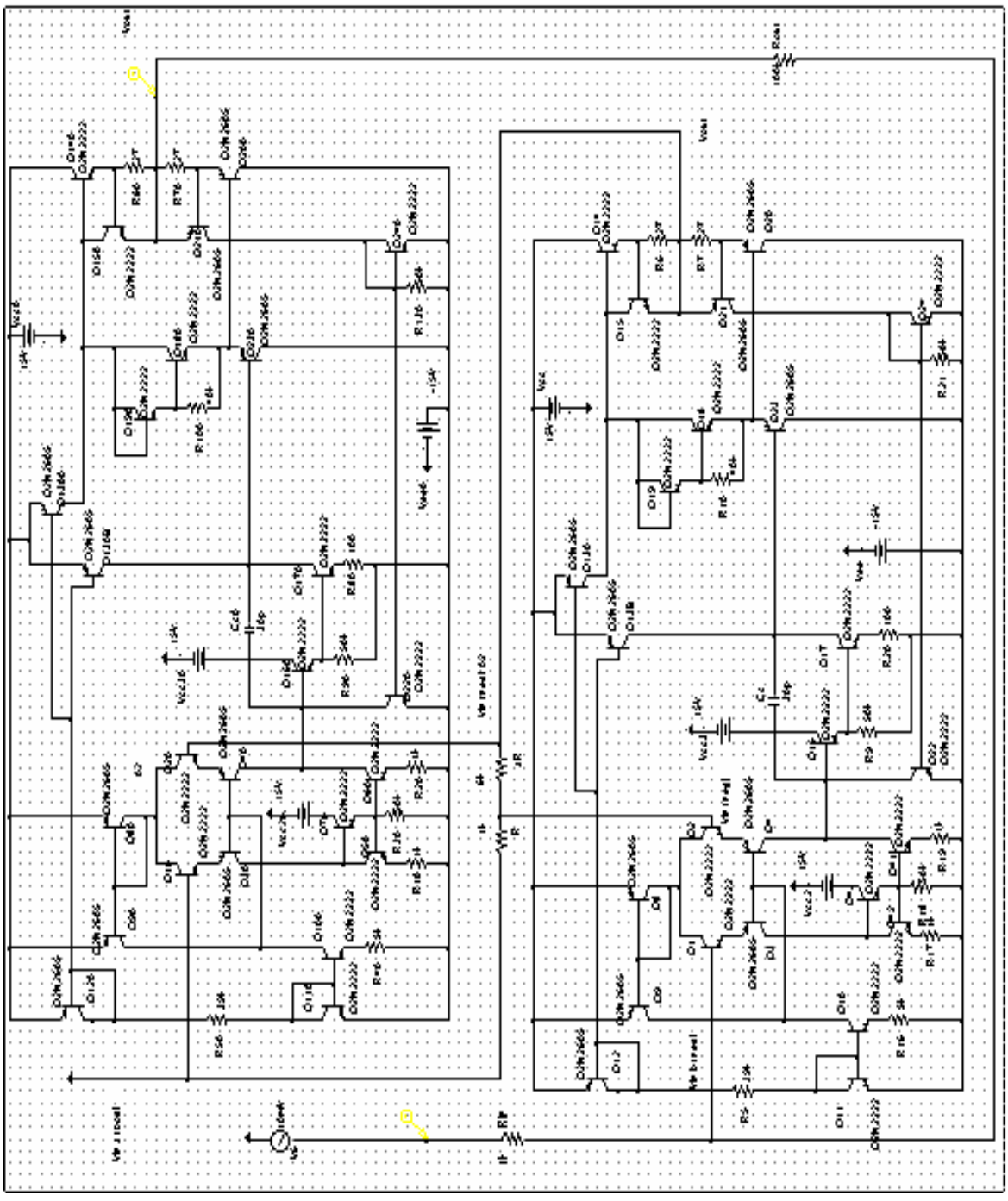

Figure 5.6. PSPICE Model of the Composite Op Amp Configured in a Finite Gain Amplifiers Circuit [From PSPICE]

E. OUTPUT BASELINE

To test if there was any validity to the simulated results, a baseline for comparison was needed. The experiments conducted by Scott Sage [Ref. 5] provided a means for comparing the simulated results. These experiments provided actual data on the effects

of total radiation dose on single and composite op amps for both rad-hardened and non-rad hardened devices. Chapter VI presents the results of this simulation and a comparison to the actual results of Sage's experiments.

THIS PAGE INTENTIONALLY LEFT BLANK

VI. RESULTS

A. OBJECTIVES

The goal of this thesis was two fold. The first objective was to simulate the effects of radiation on a single and composite op amp and produce results which could be comparable to the actual experiments, conducted at the NPS LINAC. The second objective was to confirm that the composite op amp had a higher bandwidth than that of the single op amp when irradiated.

These simulations were run while changing op amp component parameters to replicate the effects of total rad dose up to 3 Mrad (Si). The data collected from these simulations were the values and percentage changes of the gain, 3-dB frequency, and the GBWP for the single and composite op amp. These results are presented as a comparison of the performance of the single and composite op amps in Figures 6.1 through 6.6.

Figures 6.1 and 6.2 depict the simulated gain and gain percentage change for both the single and composite op amps. It can be seen that the gain for both the single and composite op amp were about equal and neither op amp experienced any degradation in gain due to a total radiation dose of 3 Mrad (Si). This concurs with Baczuk's results in Figures 5.2 and 5.3 where gain was not affected until the values of β were severely decreased.

Figures 6.3 and 6.4 compare the 3-dB frequency and 3-dB frequency percentage change for the single and composite op amp. Figure 6.3 shows that the 3-dB frequency of the composite op amp is much higher than that of the single op amp. Figure 6.4 illustrates that the 3-dB frequency for both op amps degrade at about the same percentage with respect to total dose radiation.

Figures 6.5 and 6.6 depict the GBWP and percent of change in GBWP for the single and composite op amps. For both op amps, the GBWP and their percentages of change were practically identical.

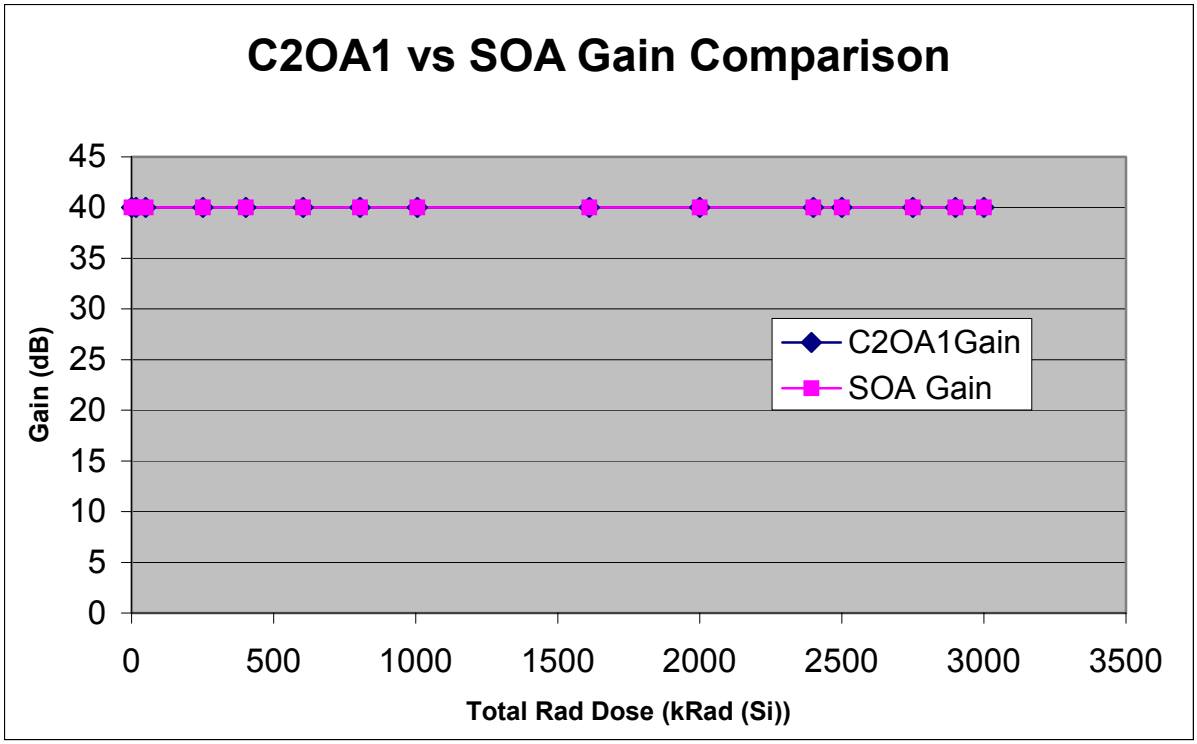

Figure 6.1. Single and Composite Op Amp Gain Comparison

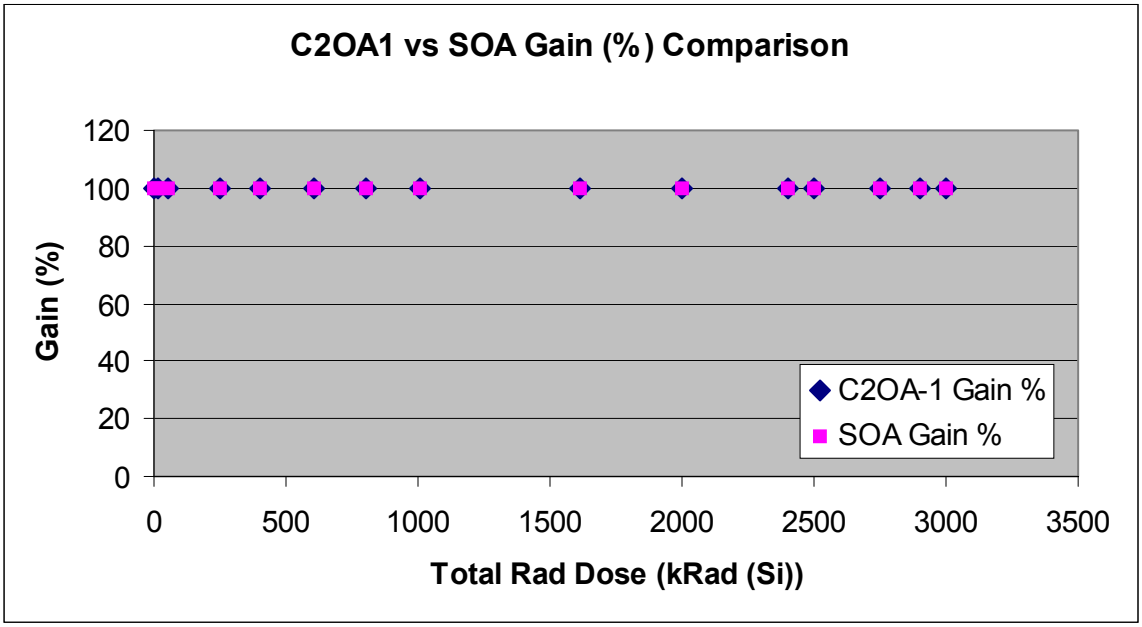

Figure 6.2. Single and Composite Op Amp Gain % Comparison.

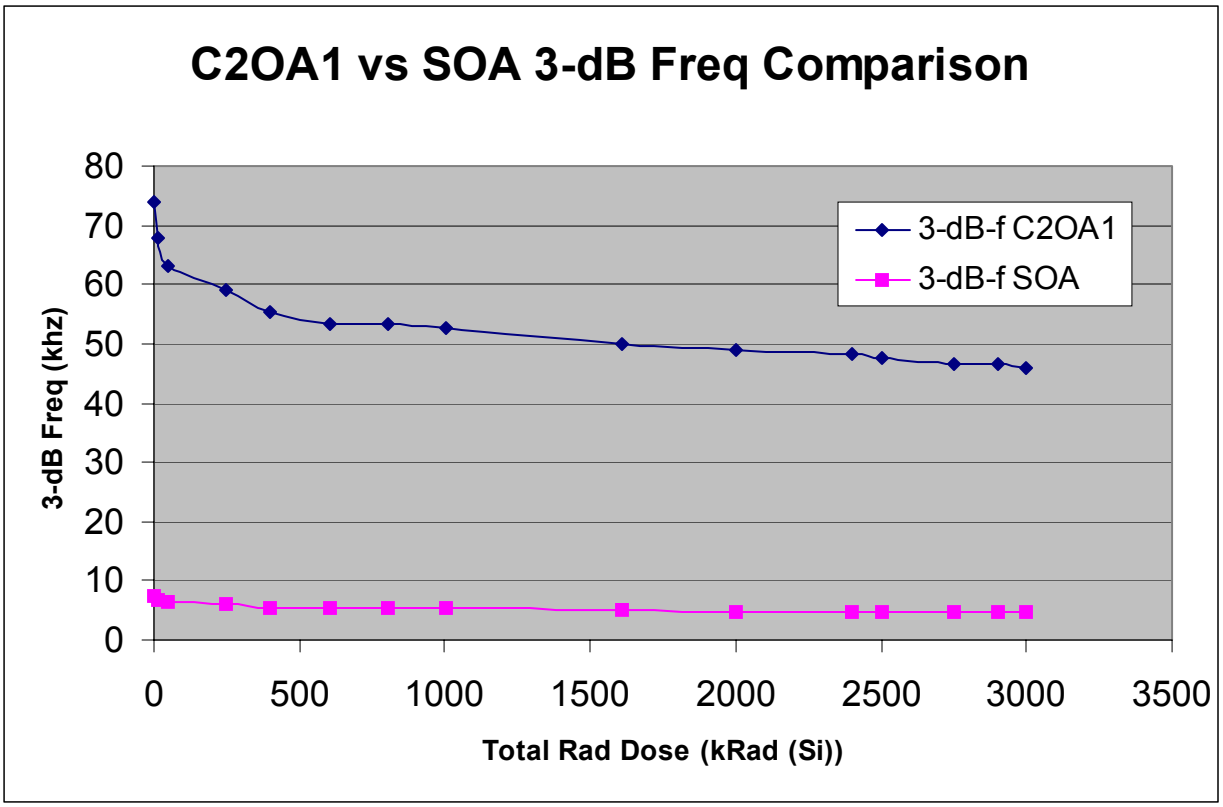

Figure 6.3. Simulated Single and Composite Op Amp 3-dB Frequency Comparison

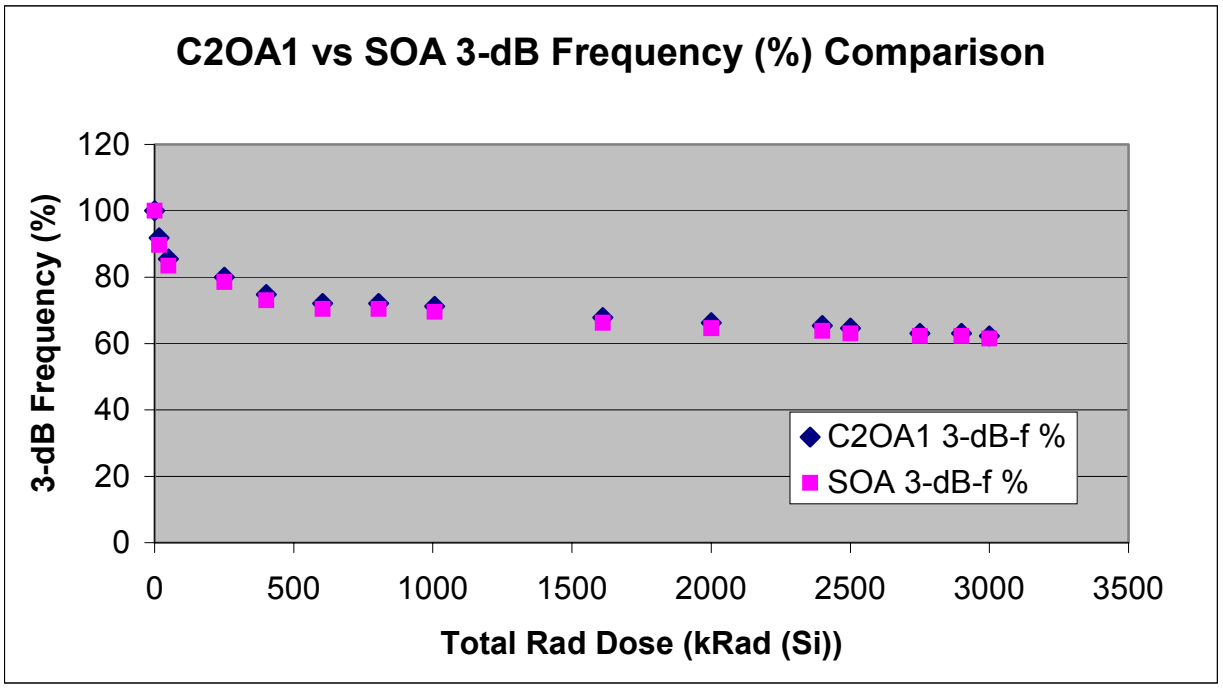

Figure 6.4. Simulated Single and Composite Op Amp 3-dB Frequency % Comparison

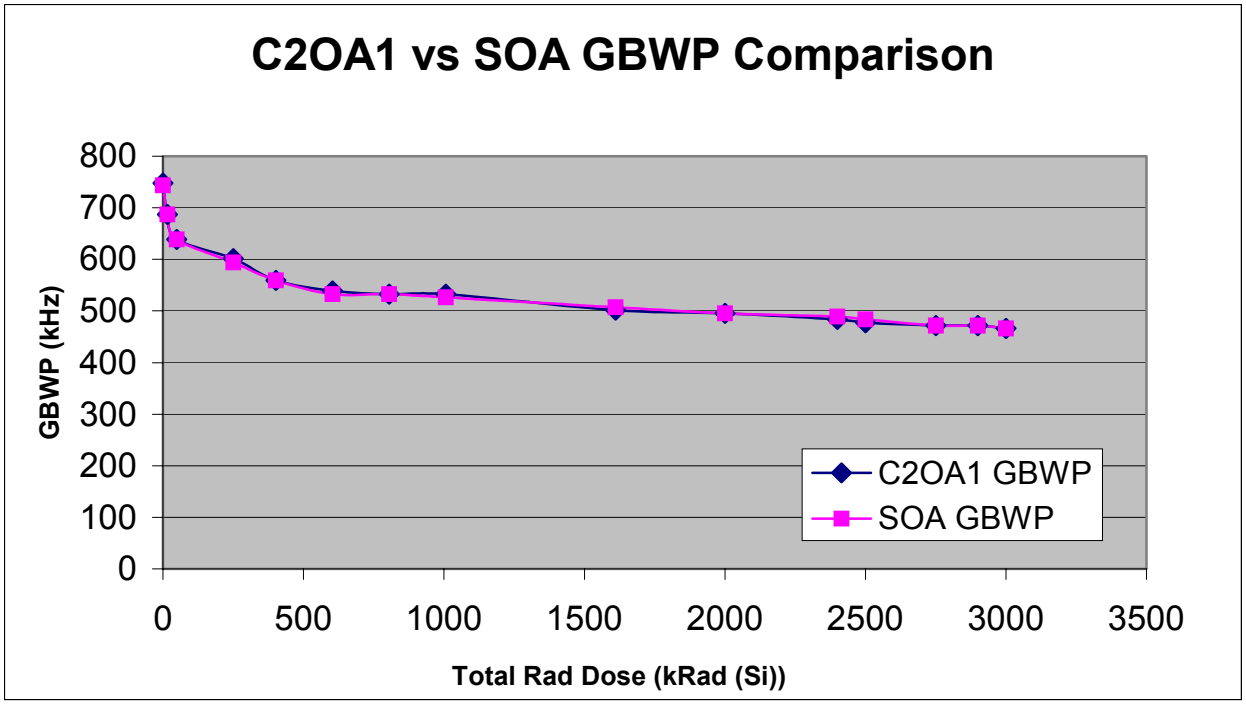

Figure 6.5. Single and Composite Op Amp Gain Bandwidth Product Comparison

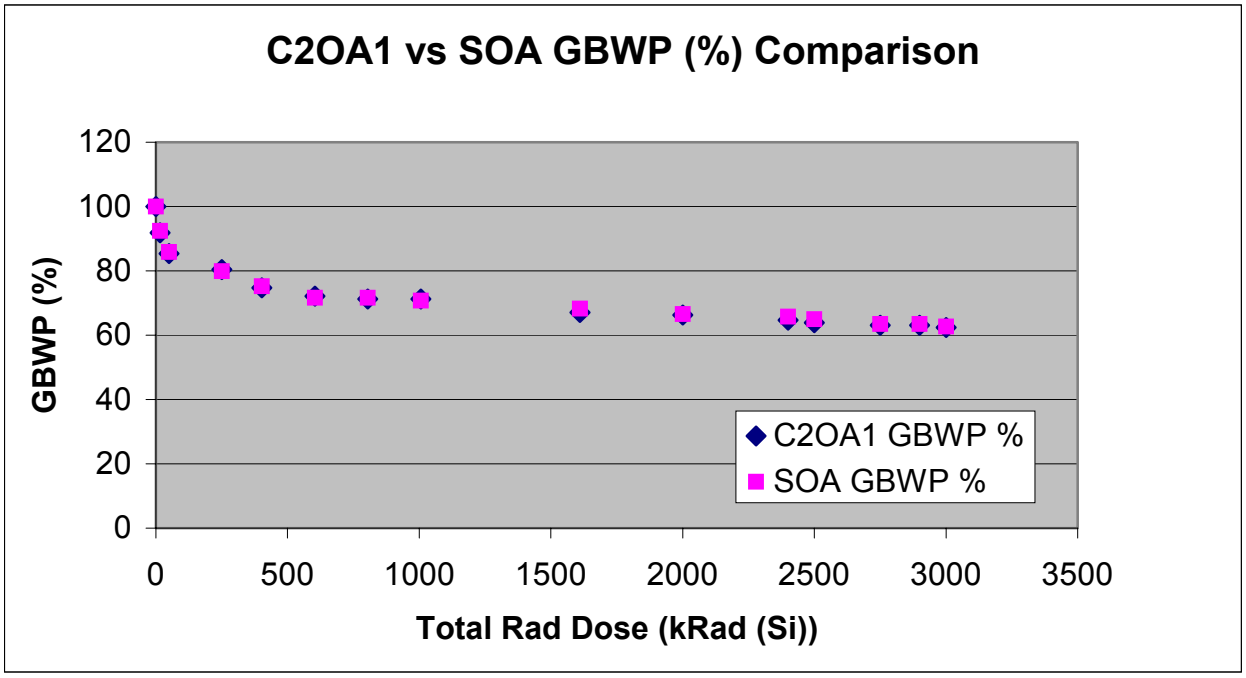

Figure 6.6. Single and Composite Op Amp Gain Bandwidth Product Percentage Comparison

B. BASELINE FOR COMPARISON

For a comparative baseline the actual results from the experiments conducted by Sage [Ref. 5] in Figures 4.9 through 4.13 considered for use. Figure 4.9 depicted the 3-dB frequency (%) of two single and one composite non-rad hardened op amps irradiated up to 6.3 Mrad (Si). Figure 4.10 depicted the gain (%) of the same op amps. Although it was desirable to compare the simulations against non-rad hardened op amps, the data available was insufficient for making a reasonable comparison.

Figure 4.11 though 4.13 depict the 3-dB frequency (%), gain (%) and 3-dB Frequency of two single and one composite radiation hardened op amps, which were irradiated up to 3 Mrad (Si). These experiments provided sufficient data points for a comparative analysis and the total rad dose for this experiment was the best match for the data available for the changes in β and capacitance values for the simulation. The raw data from these simulations were data-merged with the raw data from Sage's experiments for a comparative analysis. Comparisons with the actual experiments and the simulations are provided in Figures 6.7 through 6.12.

C. SINGLE OP AMP COMPARISON

Figures 6.7 through 6.9 show the actual and simulated single op amp comparisons, where circuits SOA 1 and SOA 2 were from the actual experiments and Sim represents the simulated circuit. Figure 6.7 shows the gain percentage comparison. From the graph it can be seen that the simulated circuit showed no decrease in gain compared to the actual circuits. Figure 6.8 and 6.9 show the 3-dB frequency and 3-dB frequency (%) change comparisons, respectively. From the graphs it can be seen that the simulated circuit results plotted higher than the actual, but it did follow a pattern similar to that of the actual results.

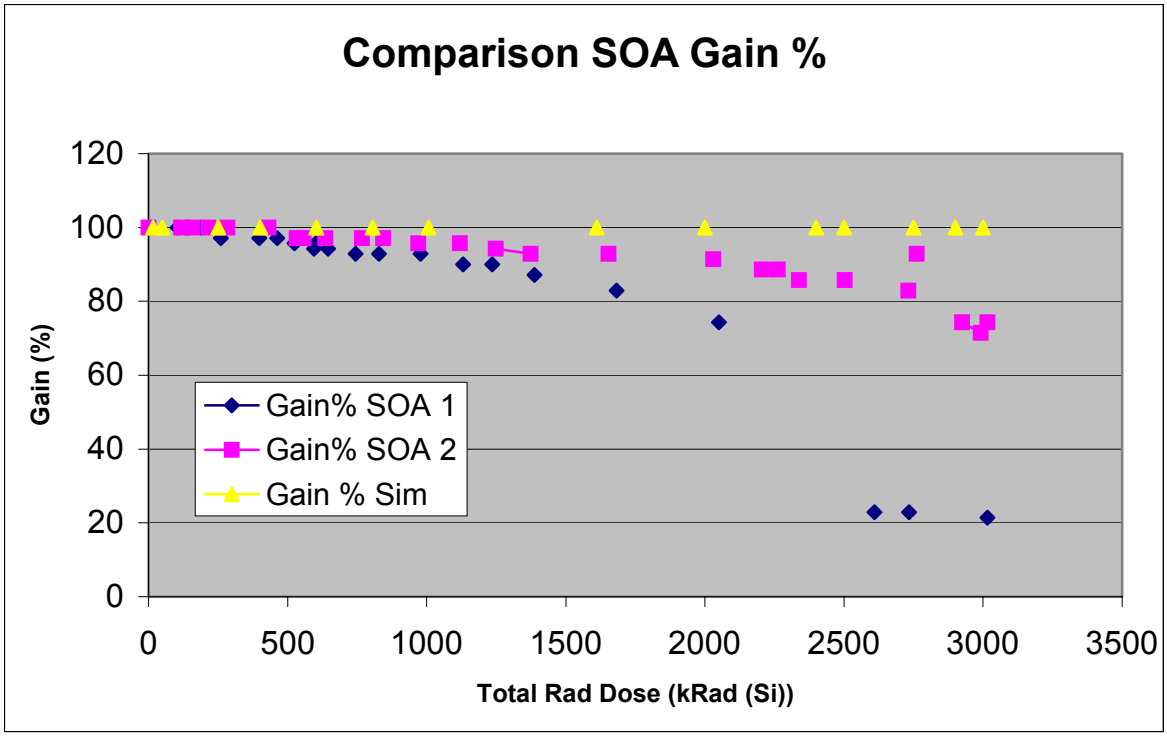

Figure 6.7. Single Op Amp Actual and Simulated Gain (%) Comparison

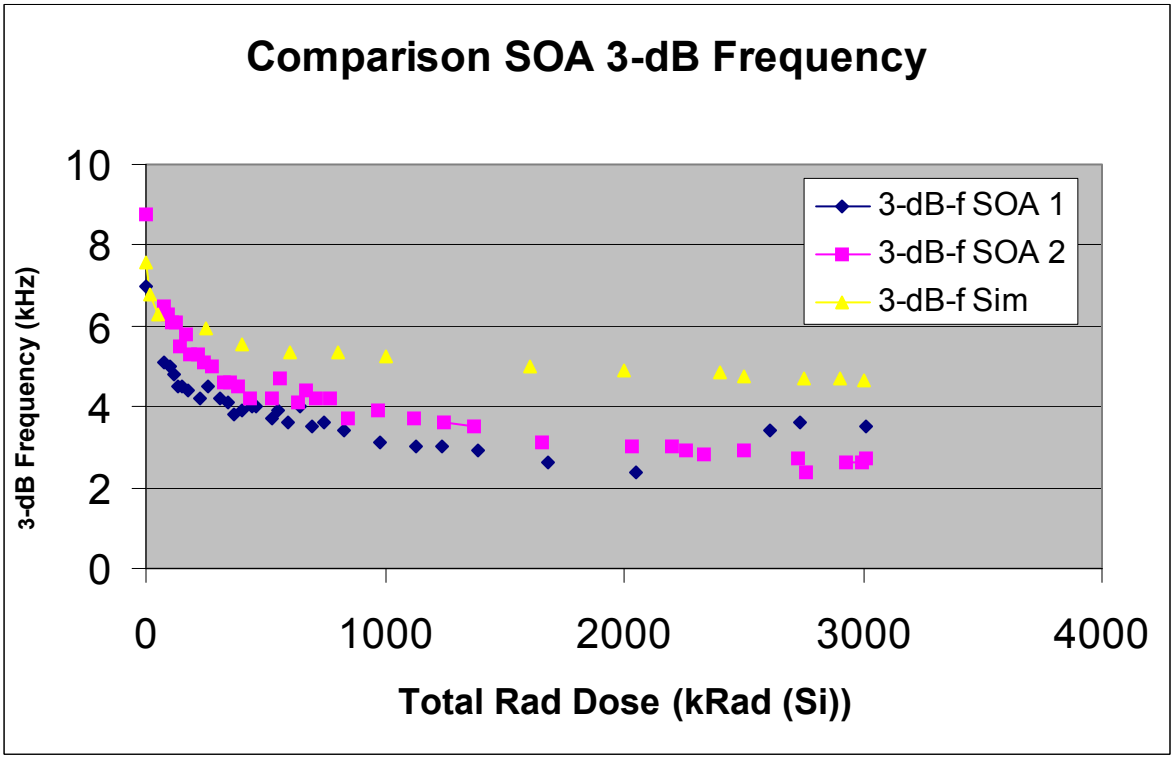

Figure 6.8. Single Op Amp Actual and Simulated 3-dB Frequency Comparison

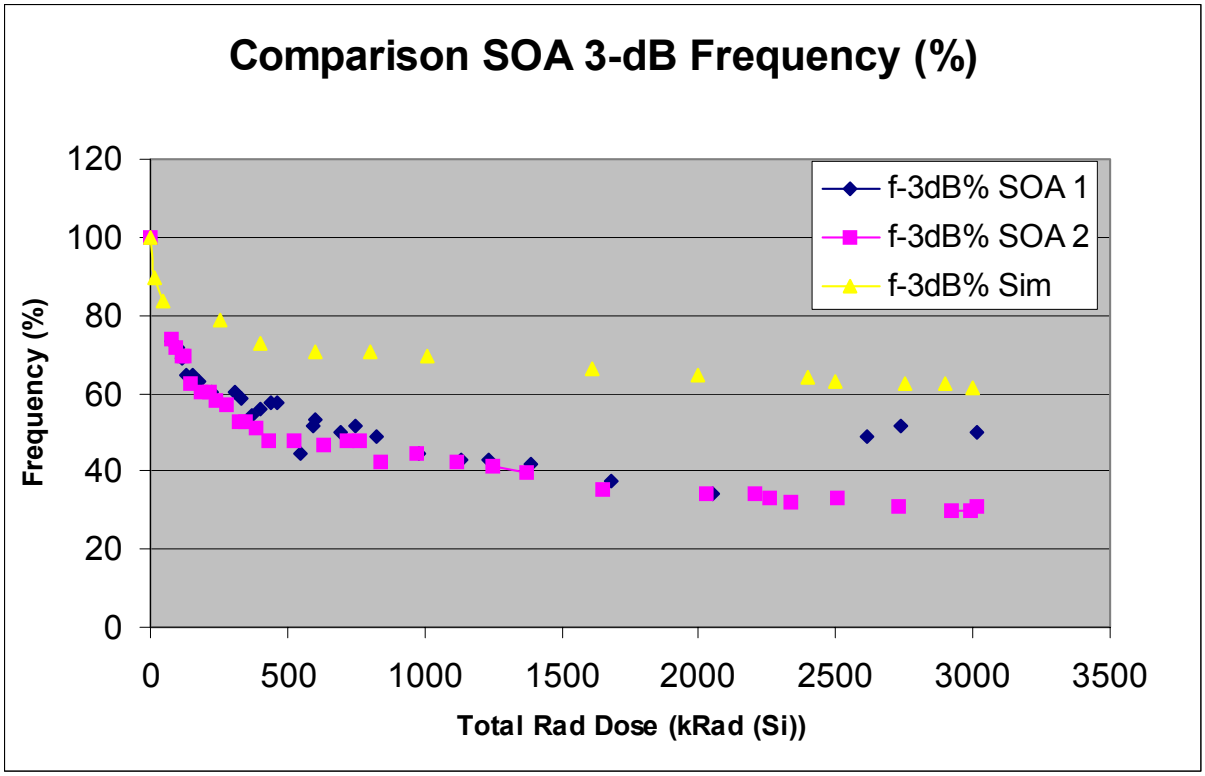

Figure 6.9. Single Op Amp Actual and Simulated 3-dB (%) Frequency Comparison

D. COMPOSITE OP AMP COMPARISON

Figures 6.10 through 6.12 show the composite op amp comparisons where the simulated circuit was compared with C2OA1 from the actual experiments. Figure 6.10 depicts the gain percentage comparison. For both circuits there was no decrease in gain seen for a total rad dose of 3 Mrad (Si), so both graphs plotted very close to each other. Figures 6.11 and 6.12 depict the 3-dB frequency and 3-dB frequency percentage change comparisons respectively. From these graphs, it can be seen that the simulated results followed very closely to the actual experiments.

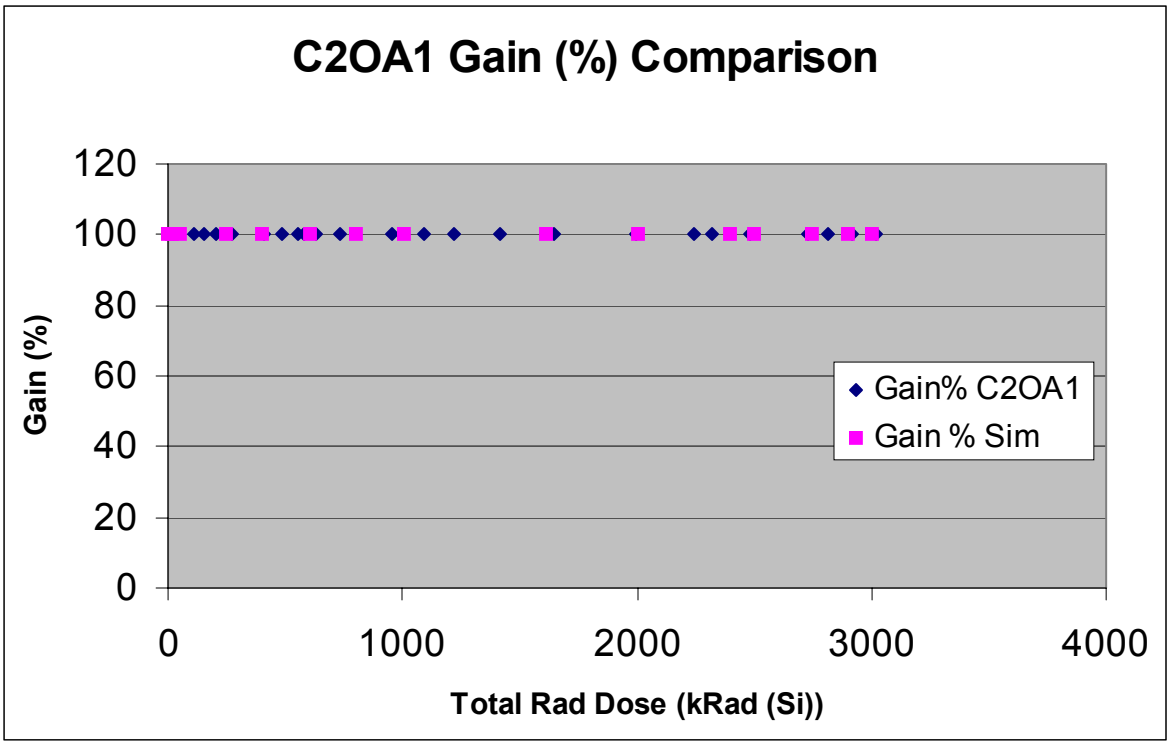

Figure 6.10. Gain Percentage Comparison for the Actual and Simulated Irradiated C2OA1

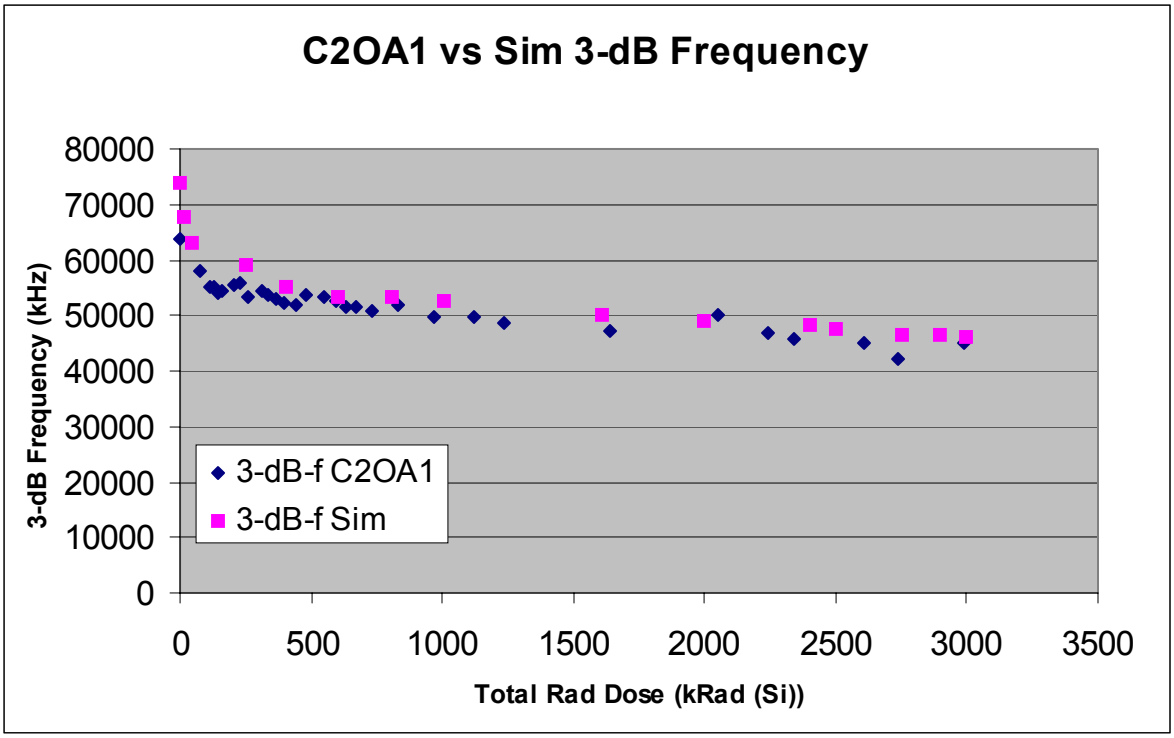

Figure 6.11. 3-dB Frequency Comparison for the Actual and Simulated Irradiated C2OA1

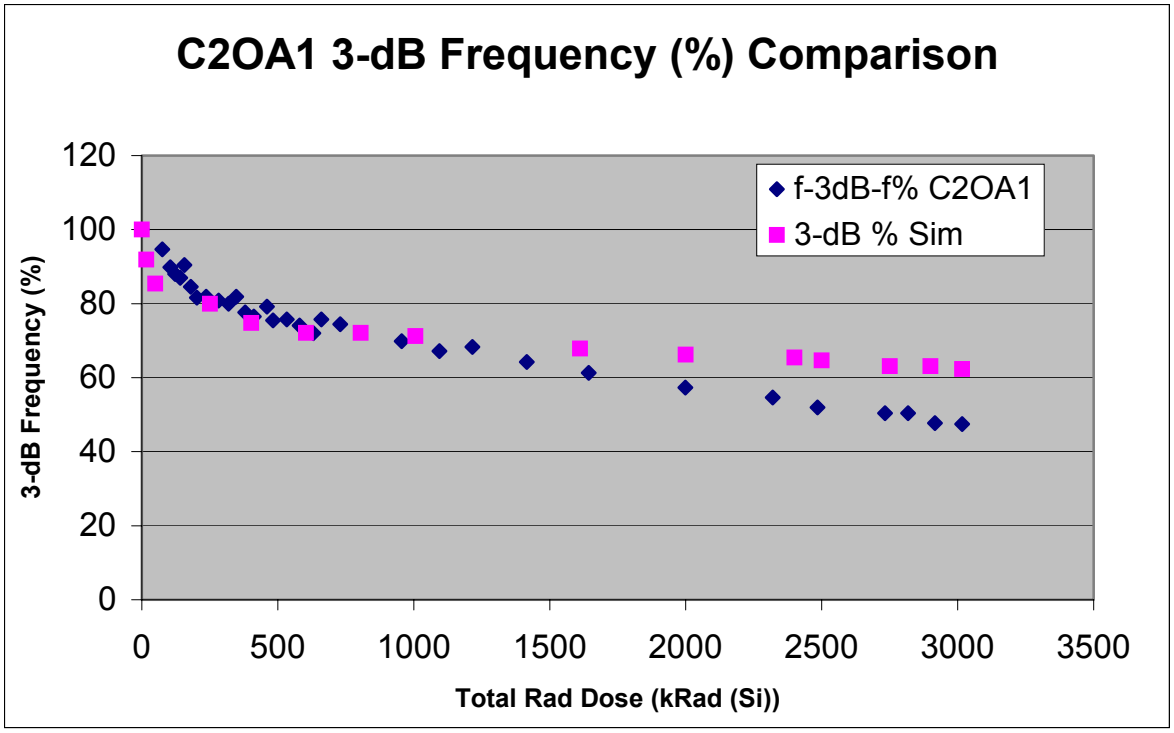

Figure 6.12. 3-dB Frequency Percentage for the Actual and Simulated C2OA-1

E. C2OA1 AND SINGLE OP AMP (SOA) COMPARISONS

The second objective of this experiment was to confirm through simulation that the composite op amp had a higher bandwidth than the single op amp when irradiated. Figures 6.13 through 6.15 provide performance comparisons for the two types of op amps. As a secondary analysis, the results of this experiment were compared with the results of the simulations conducted by Rebecca Baczuk. [Ref. 3] In Baczuk's experiments only the current gain (β) was varied and are depicted in Figures 6.13 through 6.15 as C2OA1 beta and SOA beta. In these comparisons, the β values for all four op amp circuits were varied from 0% to 50% of their original values. The capacitances of the single and composite op amps simulated in this experiment were the only other variables changed and are depicted as SOA and C2OA1.

Figure 6.13 compares the gain for all four op amps. From the graph it can be seen that both C2OA1s and both SOAs plotted very close to each other. They also showed no degradation in gain as a result of the value of β decreasing as the total dose radiation increased.

Figure 6.14 compares the 3-dB frequency for the four op amps. With this comparison, a very different result emerges. From the graph it can be seen that the 3-dB frequencies of the two C2OA1s are far greater than that of the two SOAs. But the 3-dB frequency of C2OA1 shows degradation with the increase of total rad dose where C2OA1 beta remains constant. The same result is seen with the two SOA circuits. The 3-dB frequency of SOA beta remains constant while SOA shows degradation as total rad dose increases.

Figure 6.15 compares the GBWP of the four different op amps. This comparison provides even more diverse results. From the graph, the GBWP for both C2OA1 beta and SOA beta appear to be nearly identical to each other and shows no degradation as a result of total radiation dose. The GBWP for C2OA1 and SOA also appear be nearly identical, but they both degrade as the total rad dose increases.

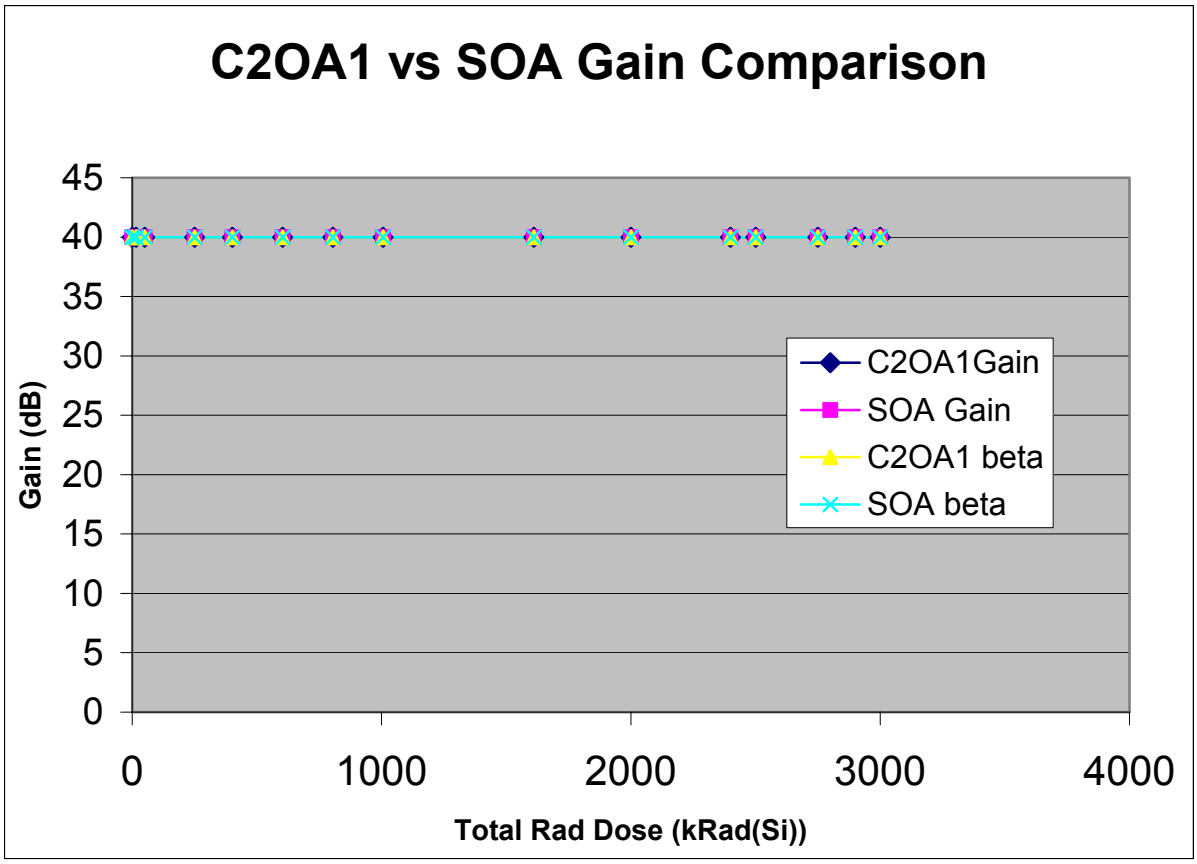

Figure 6.13. SOA and C2OA1 Gain Comparisons

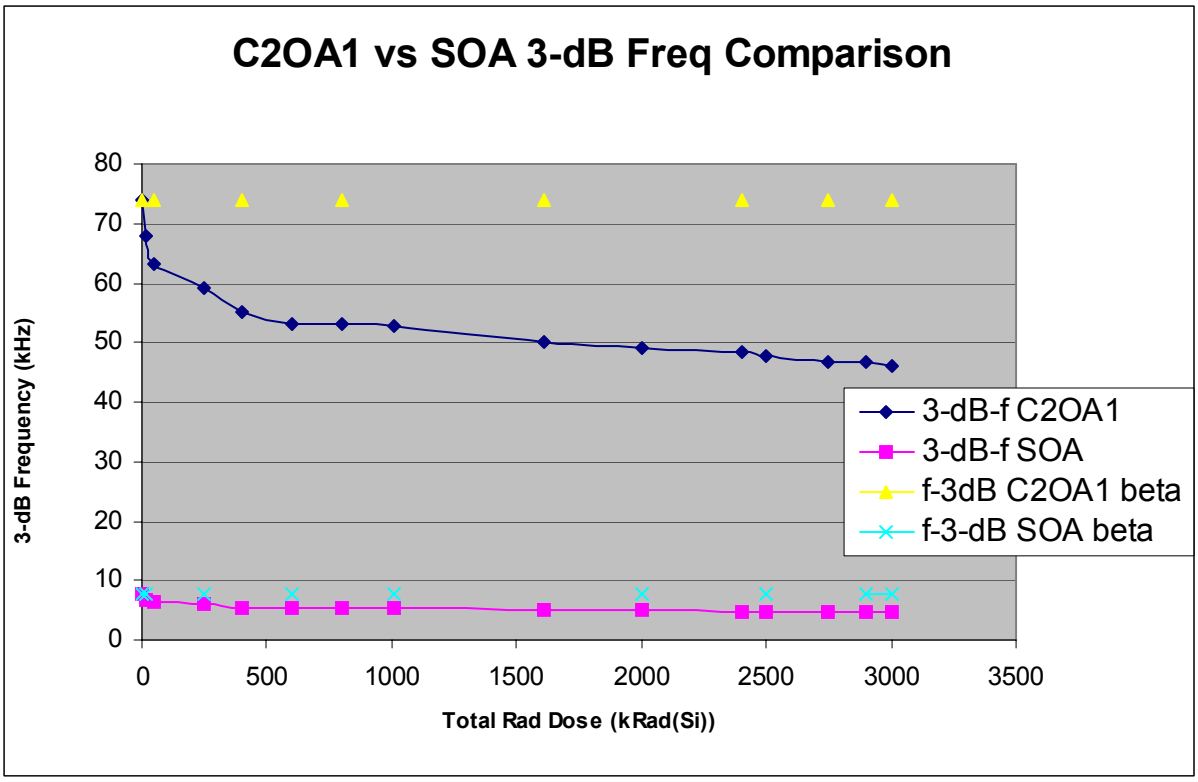

Figure 6.14. SOA and C2OA1 3-dB Frequency Comparisons

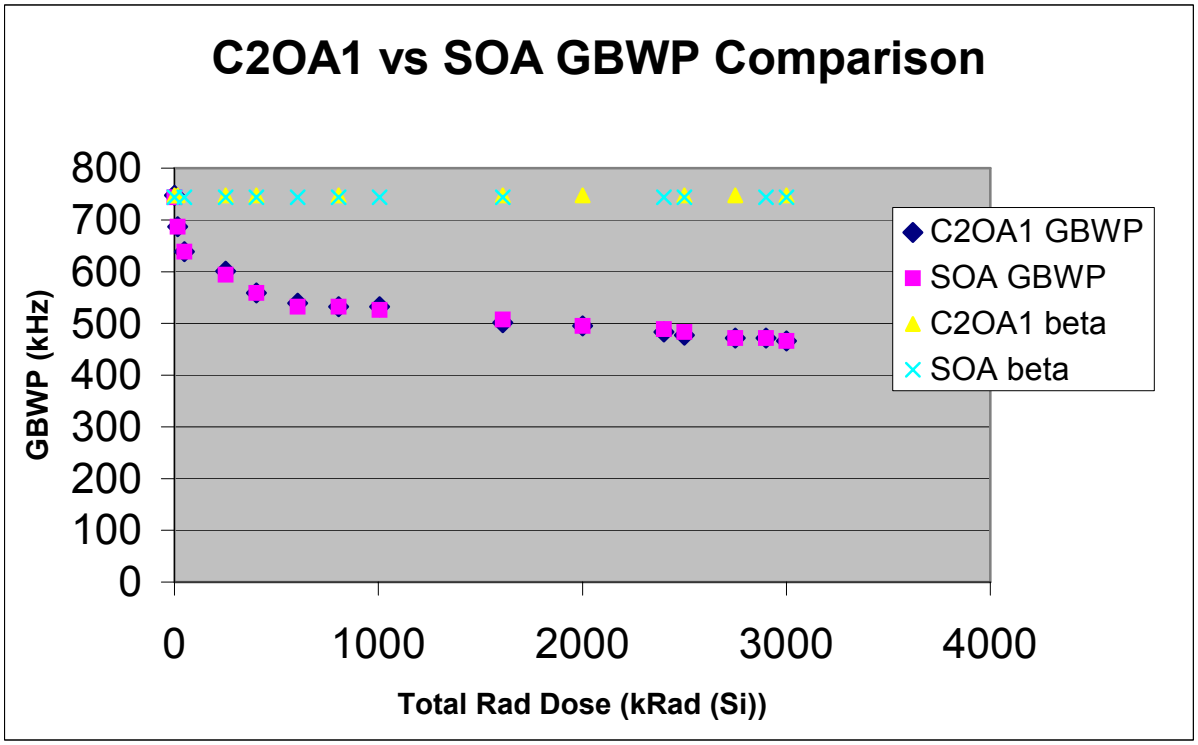

Figure 6.15. C2OA and SOA GBWP Comparison

The results of these experiments provided data that was very useful in conducting a comparative analysis of the simulated circuits with the actual irradiated circuits. Based on the results of this analysis several conclusions and recommendation were formulated. The following chapter provides these conclusions and recommendations in detail.

VII. CONCLUSIONS AND RECOMMENDATIONS

As stated in Chapter VI the objective of this thesis was two-fold. The first objective was to simulate the effects of radiation on a single and composite op amp and produce results, which could be comparable to the actual experiments, conducted at the NPS LINAC. The second objective was to confirm that the composite op amp had a higher bandwidth than that of the single op amp when irradiated.

A. SINGLE OP AMP CONCLUSIONS

The following conclusions were made from the comparative analysis conducted with the simulated SOA circuit and actual irradiated rad-hardened SOA circuits. Figure 6.7 revealed that the percentage of change in gain did not compare well with the actual data. The gain of the simulated SOA did not show any degradation due to total rad dose; the actual irradiated SOAs presented a far greater degradation in gain. This leads to a conclusion that there is another op amp variable besides that of β and capacitance value that is susceptible to the effects of total dose radiation and contributes to the overall gain of the op amp. The graphs in Figures 6.8 and 6.9 revealed that the 3-dB frequency, although higher than the actual SOA, did follow a pattern that closely resembled that of the actual SOA. From this occurrence, a hypothesis could be made that the combination of degradation in gain and the increase of capacitance as a result of total dose radiation results in the degradation of the 3-dB frequency of the SOA circuits. From this comparison, a conclusion can be made that the effect of total radiation dose on the compensating capacitor of the op amp had a major impact on the 3-dB frequency of the SOA circuit.

B. COMPOSITE OP AMP CONCLUSIONS

From the comparative analysis conducted with the simulated C2OA1 circuit and the actual irradiated rad-hardened C2OA1 circuit, the following conclusions were made. Figure 6.10 revealed that the percentage of change in gain did not change as a result of total dose radiation and plotted identically along the actual irradiated C2OA1. Although this result may be regarded as desirable, it was regarded as invalid. Since the change of gain for the simulated SOA circuit did not track with the actual SOA circuits, it was also concluded that the percent of change in gain for the simulated C2OA1 would not accurately plot with that of the actual irradiated C2OA1. However, since they both did plot

together up to 3 Mrad (Si), some other important observations were made from the comparisons. Figures 6.11 and 6.12 present the 3-dB frequency and 3-dB frequency percent of change for both simulated and actual irradiated C2OA1s. Both graphs plot remarkably close to each other. This lends credence to and supports the hypothesis that the degradation of 3-dB frequency is dependant on the total radiation dose effects on the gain and compensating capacitor of the op amp circuit.

C. SUPPORTING OBSERVATIONS

Figure 6.13 revealed that the simulated effects of radiation on the compensating capacitor had no effect on gain for both SOA and C2OA1. Both circuits plotted nearly identical to SOA beta and C2OA1 beta, respectively. Figure 6.14 showed that there was a significant difference in 3-dB frequency between C2OA1 and C2OA1 beta and SOA and SOA beta. This again supports the hypothesis that the effects of radiation on the compensating capacitor have the most significant impact on the 3-dB frequency for both C2OA1 and SOA circuits. Figure 6.15 further supports this theory. The GBWP for both SOA and C2OA1 plotted nearly identically with each other and C2OA1 beta plotted nearly identically with SOA beta. This was expected since the relationship between the GBWP and 3-dB frequency has the following relationship:

$$\omega_{3dB} = \frac{\omega_t}{1 + R_2/R_1} \tag{7.1}$$

For this equation ω_t represents the GBWP, R_2/R_1 represents the non-inverting gain of the circuit and ω_{3dB} represents the 3-dB frequency of the circuit.

D. BANDWIDTH COMPARISON OF C2OA1 AND SOA CIRCUITS

From Figure 6.13 it was shown that gain was not affected due to the increased rad dose in the SOA and C2OA1 circuits. Additionally, Figure 6.14 showed that the 3-dB frequency for the C2OA1 circuit was higher than the SOA circuits. These results are concurrent with the results obtained from previous actual and simulated experiments and thus confirm their previous conclusions.

E. RECOMMENDATIONS

From the conclusions of this study several recommendations were made to add to and aid in the continued study of the effects of radiation on single and composite operational amplifiers. The most significant recommendation made is that more experiments

on the effects of total dose radiation on non-rad hardened op amp circuits are required. The original goal of this thesis was to simulate the effects of total dose radiation on non-radiation hardened op amp circuits. The lack of sufficient data forced a comparison with rad-hardened op amp circuits. Even though these comparisons proved to be beneficial, sufficient data from non-rad hardened irradiated op amp circuits are needed to develop a PSPICE model for these op amp circuits.

A secondary recommendation is to conduct experiments with the effects of radiation on other op amp components. The results of this experiment suggested that there are other op amp component parameters that are affected by total dose radiation that were not being accounted for. It is recommended that simulated experiments be conducted to more accurately determine the effects of radiation on the gain of a single op amp and ultimately a composite op amp. Determining the op amp variables that lead to the effects of radiation on a single op amp would allow the ability to model and simulate a more accurate effect of total dose radiation.

As the need for global communications continuously increases, the greater our need for dependable satellites increase. The ability to model the effects of radiation on these electronic circuits offers opportunities, which have tremendous benefits. The cost of these circuits could be significantly lowered if their performance could be predicted at their conception rather than tested after their manufacturing. Additionally, the capability to accurately model the effects of radiation on op amp circuits prior to manufacturing would allow engineers to explore new techniques to improve their operability in the harsh environment of space and possibly extend the life of the spacecraft.

THIS PAGE INTENTIONALLY LEFT BLANK

APPENDIX. EXPERIMENT DATA

This Appendix contains all of the raw data that was used in this study. The raw data provided includes the data obtained from Salsbury's capacitor experiments, [Ref. 20] the data from Sage's op amp experiments, [Ref. 5] the data from Baczuk's simulation, [Ref. 3] and the data from the simulations conducted for this study. The raw data was used to make the graphs for comparative analysis for this thesis.

Capacitor Total Rad Dose Data (Salsbury Experiments)

Rad Dose	Capacitor 1	Capacitor 2
0	12.556	12.575
0.0169	12.64	
15.9254		13.72
39.82	14.03	
49.43		14.76
250.859		15.71
401.944		16.88
564.723	15.16	
603.399		17.55
804.854		17.74
911.341	15.68	
1006.309		17.7
1257.892	15.92	
1610.724		18.77
2399.779		19.41

Chip #2

Rad Dose	Cap Value	% Change
0	12.575	
15.9254	13.72	9.1
49.43	14.76	7.58
250.859	15.71	6.44
401.944	16.88	7.45
603.399	17.55	3.97
804.854	17.75	1.14
1006.309	17.7	0.28
1610.724	18.77	6.05
2000	19.16148	2.1
2399.779	19.41	1.3
2500	19.65123	1.24
2750	19.97629	1.68
2900	20.04878	0.35
3000	20.22956	0.9

The last five data points are forecasts

Rad Dose	Forcast Cap Values
0	30
15.9254	32.73
49.43	35.21
250.859	37.48
401.944	40.27
603.399	41.87
804.854	42.35
1006.309	42.47
1610.724	45.04
2000	45.99
2399.779	46.59
2500	47.17
2750	47.96
2900	48.13
3000	48.56

Rad Dose	Test #2	Comp Capacitor
0	12.575	30
15.9254	13.72	32.73
49.43	14.76	35.21
250.859	15.71	37.48
401.944	16.88	40.27
603.399	17.55	41.87
804.854	17.75	42.35
1006.309	17.7	42.47
1610.724	18.77	45.04
2000	19.16148	45.99
2399.779	19.41	46.59
2500	19.65123	47.17
2750	19.97629	47.96
2900	20.04878	48.13
3000	20.22956	48.56

	Raw Data from Sage's Experiment conducted on 4/18/1988 on SOA and C2OA1											
The percentage of change in 3-dB									3-dB Frequency Data from SOA and C2OA1			
Frequency for SOA and C2OA1					Percentage of change in Gain							
Rad Dose	f-3dB#1%	f-3dB#2%	f-3dB#3%	Rad Dose	Gain #1%	Gain #2%	Gain #3%	Rad Dose	3-dB Freq#2	3-dB Freq#1	3-dB Freq#3
0	100	100	100	0	100	100	100	0	63.9	6.98	8.77
75	73.066	94.67	74.116	75				75	57.88462	5.1	6.5
84				84				84			
91			71.836	91				91			6.3
97	71.633			97				97		5	
105		89.867		105	100			105			
112			69.555	112		100		112	55		6.1
117	68.768			117			100	117		4.8	
122		88		122				122			
127			69.555	127				127	55.3		6.1
132	64.47			132				132		4.5	
141		86.933		141				141			
145			62.714	145	100			145	54		5.5
151	64.47			151		100		151		4.5	
157		90.4		157			100	157	54.3		
167				167				167			5.8
174	63.037			174				174		4.4	
180		84.533		180				180			
187			60.433	187	100			187			5.3
203		81.6		203		100		203	55.5		
215			60.433	215			100	215			5.3
227	60.172			227				227	56	4.2	
236		81.867		236				236			
240			58.153	240				240			5.1
260				260	97.143			260	53.2	4.5	
274			57.013	274		100		274			5
283		80.8		283			100	283			
309	60.172			309				309	54.4	4.2	
319		80		319				319			
327			52.452	327				327			4.6
334	58.739			334				334	53.7		
347		81.867		347				347		4.1	
350			52.452	350				350			4.6
369	54.441			369				369	52.8	3.8	
380		77.6		380				380			
387			51.311	387				387			4.5
398	55.874			398	97.143			398	52.1	3.9	
412		76.533		412		100		412			
431			47.891	431			100	431			4.2

	Raw Data from Sage's Experiment conducted on 4/18/1988 on SOA and C2OA1											
The percentage of change in 3-dB									3-dB Frequency Data from SOA and C2OA1			
Frequency for SOA and C2OA1					Percentage of change in Gain							
Rad Dose	f-3dB#1%	f-3dB#2%	f-3dB#3%	Rad Dose	Gain #1%	Gain #2%	Gain #3%	Rad Dose	3-dB Freq#2	3-dB Freq#1	3-dB Freq#3
442	57.307			442				442	51.73846	4	
460		79.2		460				460			
463	57.307			463	97.143			463		4	
482		75.467		482		100		482	53.8		
525			47.891	525	95.714			525		3.7	4.2
533		75.733		533			97.143	533			
551	44.47			551		100		551	53.2	3.9	
558				558			97.143	558			4.7
580		74.133		580		100		580			
595	51.576			595	94.286			595	52.5	3.6	
602	53.009			602	95.714			602			
631		72		631		100		631			
635			46.75	635			97.143	635	51.5		4.1
646				646	94.286			646		4	
660		75.733		660				660			
671				671				671	51.5		4.4
697	50.143			697				697		3.5	
715			47.891	715				715			4.2
730		74.4		730		100		730	50.8		
744	51.576			744	92.857			744		3.6	
767			47.891	767			97.143	767			4.2
828	48.711			828	92.857			828	51.8	3.4	
843			42.189	843			97.143	843			3.7
956		69.867		956		100		956			
970			44.47	970			95.714	970	49.78974		3.9
978	44.413			978	92.847			978		3.1	
1094		67.2		1094		100		1094			
1119			42.189	1119			95.714	1119	49.6923		3.7
1131	42.98			1131	90			1131		3	
1216		68.267		1216		100		1216			
1236	42.98			1236	90			1236	48.5231	3	
1248			41.049	1248			94.286	1248			3.6
1374			39.909	1374			92.857	1374			3.5
1387	41.547			1387	87.143			1387		2.9	
1416		64.267		1416		100		1416			
1643		61.333		1643		100		1643	47.2564		
1653			35.348	1653			92.857	1653			3.1
1682	37.249			1682	82.857			1682		2.6	
2998		57.333		2998		100		1998			

	Raw Data from Sage's Experiment conducted on 4/18/1988 on SOA and C2OA1											
The percentage of change in 3-dB								3-dB Frequency Data from SOA and C2OA1				
Frequency for SOA and C2OA1					Percentage of change in Gain							
Rad Dose	f-3dB#1%	f-3dB#2%	f-3dB#3%	Rad Dose	Gain #1%	Gain #2%	Gain #3%	Rad Dose	3-dB Freq#2	3-dB Freq#1	3-dB Freq#3
2030			34.208	2030			91.429	2030			3
2050	34.384			2050	74.286			2050	50.17949	2.4	
2205			34.208	2205			88.571	2205			3
2219				2219				2219			
2244				2244		100		2244	46.67179		
2262			33.067	2262			88.571	2262			2.9
2320		54.667		2320		100		2320			
2338			31.927	2338			85.714	2338	45.79487		2.8
2484		52		2484		100		2484			
2502			33.067	2502			85.714	2502			2.9
2610	48.711			2610	22.857			2610	45.01538	3.4	
2731			30.787	2731			82.857	2731			2.7
2733		50.4		2733		100		2733			
2734	51.576			2734	22.857			2734	41.99487	3.6	
2761				2761			92.857	2761			2.4
2818		50.4		2818		100		2818			
2916		47.733		2916		100		2916			
2925			29.647	2925			74.286	2925			2.6
2992			29.647	2992			71.429	2992	45.2		2.6
3016	50.143	47.467	30.787	3016	21.429	100	74.286	3016		3.5	2.7

Simulation Comparisons

Gain Comparisons for Simulated SOAs and C2OA1s

Rad Dose	C2OA-1Ga	SOA Gain	C2OA1 bet	SOA beta
0	39.999	39.995	39.999	39.995
15.9254	39.999	39.995	39.999	39.995
49.43	39.999	39.995	39.999	39.995
250.859	39.999	39.995	39.999	39.995
401.944	39.999	39.995	39.999	39.995
603.399	39.999	39.995	39.999	39.995
804.854	39.999	39.995	39.999	39.995
1006.309	39.999	39.995	39.999	39.995
1610.724	39.999	39.995	39.999	39.995
2000	39.999	39.995	39.999	39.995
2399.779	39.999	39.995	39.999	39.995
2500	39.999	39.995	39.999	39.995
2750	39.999	39.995	39.999	39.995
2900	39.999	39.995	39.999	39.995
3000	39.999	39.995	39.999	39.995

3-dB Frequency Comparisons for Simulated SOAs and C2OA1s

Rad Dose	3-dB-f C2C	3-dB-f SOA	f-3dB C2O	f-3-dB SOA beta
0	73.862	7.567	73.862	7.567
15.9254	67.855	6.7855		7.567
49.43	63.096	6.3096	73.862	
250.859	59.04	5.9386		7.567
401.944	55.221	5.527	73.862	
603.399	53.25	5.325		7.567
804.854	53.25	5.325	73.862	
1006.309	52.608	5.2608		7.567
1610.724	50.119	5.0119	73.862	
2000	48.919	4.8919		7.567
2399.779	48.329	4.8329	73.862	
2500	47.747	4.7747		7.567
2750	46.604	4.7172	73.862	
2900	46.604	4.7172		7.567
3000	46.042	4.6604	73.862	7.567

GBWP Comparisons for Simulated SOAs and C2OA1s

Rad Dose	C2OA1 GB	SOA GBW	C2OA1 bet	SOA beta
0	747.626	743.551	747.626	743.551
15.9254	686.819	686.819	747.626	
49.43	638.65	638.65		743.551
250.859	601.101	593.86	747.626	743.551
401.944	558.944	558.944	747.626	743.551
603.399	538.988	532.495		743.551
804.854	532.495	532.495	747.626	743.551
1006.309	532.495	526.081		743.551
1610.724	501.187	507.298	747.626	743.551
2000	495.15	495.15	747.626	
2399.779	483.293	489.186		743.551
2500	477.471	483.293	747.626	743.551
2750	471.72	471.72	747.626	
2900	471.72	471.72		743.551
3000	466.038	466.038	747.626	743.551

Raw Data from SOA Simulations

Rad Dose	3-dB Freq	3-dB Freq	Gain	Gain %	GBWP	GBWP %	Cap Values
0	7.567	7.567	39.995	100	743.551	100	30
15.9254	6.7855	6.7855	39.995	100	686.819	92.4	32.73
49.43	6.3096	6.3096	39.995	100	638.65	85.9	35.21
250.859	5.9386	5.9386	39.995	100	593.86	79.9	37.48
401.944	5.527	5.527	39.995	100	558.944	75.2	40.27
603.399	5.325	5.325	39.995	100	532.495	71.62	41.87
804.854	5.325	5.325	39.995	100	532.495	71.62	42.35
1006.309	5.2608	5.2608	39.995	100	526.081	70.75	42.47
1610.724	5.0119	5.0119	39.995	100	507.298	68.23	45.04
2000	4.8919	4.8919	39.995	100	495.15	66.6	45.99
2399.779	4.8329	4.8329	39.995	100	489.186	65.8	46.59
2500	4.7747	4.7747	39.995	100	483.293	65	47.17
2750	4.7172	4.7172	39.995	100	471.72	63.44	47.96
2900	4.7172	4.7172	39.995	100	471.72	63.44	48.13
3000	4.6604	4.6604	39.995	100	466.038	62.68	48.56

Raw Data from C2OA1 Simulations

Rad Dose	3-dB Frequ	3-dB Freq	Gain	Gain %	GBWP	GBWP %	Cap Values
0	73.862	100	39.999	100	747.626	100	30
15.9254	67.855	91.87	39.999	100	686.819	91.87	32.73
49.43	63.096	85.42	39.999	100	638.65	85.42	35.21
250.859	59.04	79.93	39.999	100	601.101	80.4	37.48
401.944	55.221	74.76	39.999	100	558.944	74.76	40.27
603.399	53.25	72.1	39.999	100	538.988	72.1	41.87
804.854	53.25	72.1	39.999	100	532.495	71.22	42.35
1006.309	52.608	71.22	39.999	100	532.495	71.22	42.47
1610.724	50.119	67.85	39.999	100	501.187	67.04	45.04
2000	48.919	66.23	39.999	100	495.15	66.23	45.99
2399.779	48.329	65.43	39.999	100	483.293	64.64	46.59
2500	47.747	64.64	39.999	100	477.471	63.86	47.17
2750	46.604	63.1	39.999	100	471.72	63.1	47.96
2900	46.604	63.1	39.999	100	471.72	63.1	48.13
3000	46.042	62.34	39.999	100	466.038	62.34	48.56

THIS PAGE INTENTIONALLY LEFT BLANK

LIST OF REFERENCES

1. Columbia Electronic Encyclopedia, "Hubble Space Telescope,, [www.infoplease.com/ce6/sci/A0824422.html], last accessed 24 May 2004.

2. Rivet, S., *Space Radiation Environments*, Harris Semiconductor, Melbourne, Florida, September 1993.

3. Baczuk, Rebecca L., *Pspice Simulation of Total Dose Effects on Composite and Single Operational Amplifiers*, Master's Thesis, Naval Postgraduate School, Monterey, California, September 1994.

4. Sedra, A. S. and Smith, K. C., *Microelectronic Circuits*, 4th ed., Oxford University Press, Oxford 1998.

5. Sage, Scott E., *Total Dose Radiation Effects on Bipolar Composite and Single Operational Amplifiers Using a 30 MeV Linear Accelerator*, Master's Thesis, Naval Postgraduate School, Monterey, California, June 1988.

6. Griffin, Noel, "Radiation Protection Training Course," [www.triumf.ca/safety/rpt/rpt.html], 1996, last accessed 06 April 2004.

7. *Wikipedia*, "Wikipedia Online Encyclopedia," Wikipedia Foundation, 2001, [http://en.wikipedia.org/wiki/Radiation], last accessed 06 April 04.

8. Messenger, G. S. and Ash, M. S., *The Effects of Radiation on Electronic Systems*, Van Nostrand Reinhold Company, New York, 1986.

9. Hess, Wilmot N., *The Radiation Belt and Magnetosphere*, Blaisdell Publishing, Waltham, Massachusetts, 1968.

10. National Oceanographic and Atmospheric Administration, "Cosmic Rays," NOAA, [www.noaa.gov], last accessed 06 April 2004.

11. Mewaldt, R. A., "Cosmic Rays," *Macmillian Encyclopedia of Physics*, California Institute of Technology, 1996, [www.srl.caltech.edu/personnel/dick/cos_encyc.html], last accessed 03 April 04.

12. Corliss, W. R., *Space Radiation*, United States Atomic Energy Commission, Commission Office of Information Services, 1968.

13. Hughes, David B., "The Plasma Universe," New Science Paradigms, [www.newscienceparadigms.com/astro/plasma universe.htm], last accessed 06 April 2004.

14. Green, James L., "The Magnetosphere," NASA Goddard Space flight Center, [ssdoo.gsfc.nasa.gov/education/lectures/magnetosphere.html], last accessed 06 April 2004.

15. Larin, Frank, *Radiation Effects in Semiconductor Devices*, John Wiley and Sons Inc., New York, 1968.

16. Rudie, Norman J., *Principles and Techniques of Radiation Hardening*, Vols. III, IV, and V, Western Periodicals Co., North Hollywood, California, 1986.

17. Brittain, Donald R., *Total Dose Radiation Effects on Hardened SOI Bipolar Transistors Using the NPS LINAC*, Master's Thesis, Naval Postgraduate School, Monterey, California, March 1995.

18. Carlson, A. B., *Circuits; Engineering Concepts and Analysis of Linear Electric Circuits*, Thomas Learning, Brooks/Cole, Pacific Grove, California, 1986.

19. Abrahamson, Stuart M., *In-Situ Measurement of Total Dose Radiation Effects on Parallel Plate MOS Capacitors Using the NPS Linear Accelerator*, Master's Thesis, Naval Postgraduate School, Monterey, California, December, 1995.

20. Salsbury, Duane, *In-situ testing of Radiation Effects on VLSI Capacitors Using the NPS Linear Accelerator*, Master's Thesis, Naval Postgraduate School, Monterey, California, December 1996.

21. Harris Corporation, "Analog Product Data Book," Harris Corporation, Melbourne, Florida, 1986.

22. Michael, Sherif and Mikhael, Wasfy B., "Inverting Integrator and Active Filter Applications of Composite Operational Amplifiers," *IEEE Transistor Circuits and Systems*, CAS-34, No. 5, pp. 449-460, May 1987.

23. Michael, Sherif and Mikhael, Wasfy B., "Composite Operational Amplifiers: Generation and Finite Gain Applications," *IEEE Transistor Circuits and Systems*, CAS-34, No. 5, pp. 449-460, May 1987.

24. Lohr, David Michael, *A Technique for Improving Active Network Performance in a Radiation Environment Without the Use of Hardened Devices*, Master's Thesis, Naval Postgraduate School, Monterey, California, March 1987.

25. Lambeth, Benjamin S., "Footing the Bill for Military Space," *Air Force Magazine, Journal of the Air Force Association*, Vol. 86, No. 8, August 2003.

26. Van Zeghbroeck, B., "Principles of Semiconductor Devices," [www.colorado.edu/~bart/book], last accessed 02 May04.

27. Andrus, Jeremy, “The 741 Op Amp, DC and Small Signal Analysis,” Calvin University, [engr.calvin.edu/PRibeiro_WEBPAGE/courses/engr332/ Handouts/ 741 opAmp.ppt], last accessed 10 May 04

THIS PAGE INTENTIONALLY LEFT BLANK

INITIAL DISTRIBUTION LIST

1. Defense Technical Information Center
   Ft. Belvoir, Virginia

2. Dudley Knox Library
   Naval Postgraduate School
   Monterey, California

3. Chairman, Code EC
   Department of Electrical and Computer Engineering
   Naval Postgraduate School
   Monterey, California

4. Professor Sherif Michael, Code EC
   Department of Electrical and Computer Engineering
   Naval Postgraduate School
   Monterey, California

5. Professor Andrew Parker, Code EC
   Department of Electrical and Computer Engineering
   Naval Postgraduate School
   Monterey, California

6. David M. Dufour
   New Orleans, Louisiana